U.S. DEPARTMENT OF COMMERCE

PB80-169576

Dispersion of Sulfur Dioxide from the Clinch River Power Plant, A Wind-Tunnel Study

(U.S.) Environmental Sciences Research Lab.
Research Triangle Park, NC

Sep 79

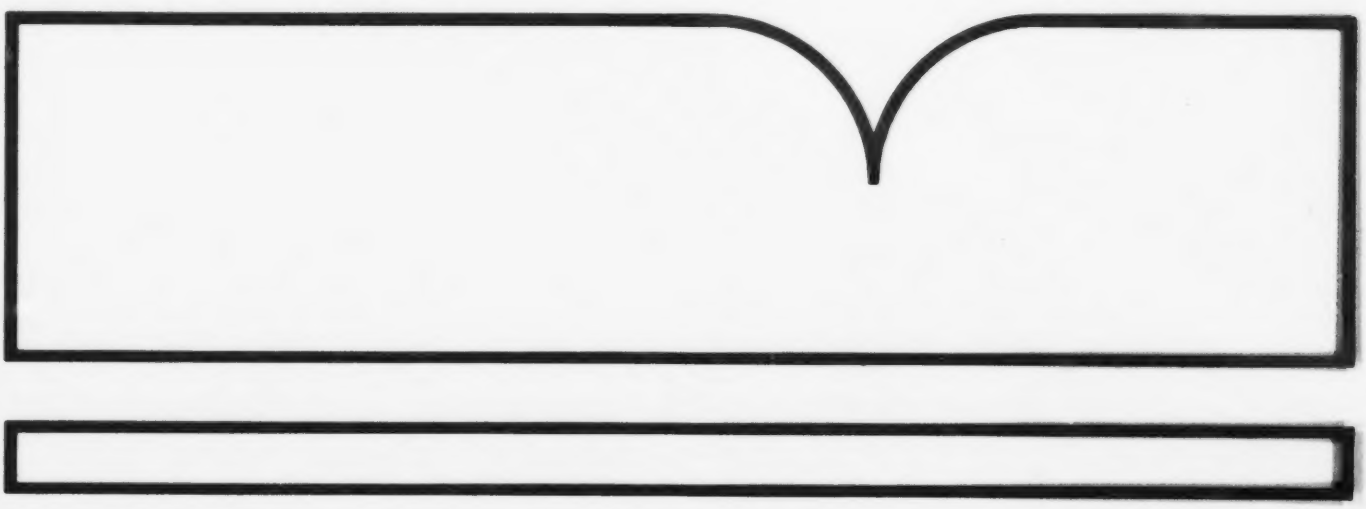

U.S. Department of Commerce
National Technical Information Service
NTIS

United States
Environmental Protection
Agency

Environmental Sciences Research
Laboratory
Research Triangle Park NC 27711

EPA-600/4-79-052
September 1979

Research and Development

PB80-169576

EPA

Dispersion of Sulfur Dioxide from the Clinch River Power Plant

A Wind-Tunnel Study

REPRODUCED BY
NATIONAL TECHNICAL
INFORMATION SERVICE
U. S. DEPARTMENT OF COMMERCE
SPRINGFIELD, VA. 22161

RESEARCH REPORTING SERIES

Research reports of the Office of Research and Development, U.S. Environmental Protection Agency, have been grouped into nine series. These nine broad categories were established to facilitate further development and application of environmental technology. Elimination of traditional grouping was consciously planned to foster technology transfer and a maximum interface in related fields. The nine series are:

1. Environmental Health Effects Research
2. Environmental Protection Technology
3. Ecological Research
4. Environmental Monitoring
5. Socioeconomic Environmental Studies
6. Scientific and Technical Assessment Reports (STAR)
7. Interagency Energy-Environment Research and Development
8. "Special" Reports
9. Miscellaneous Reports

This report has been assigned to the ENVIRONMENTAL MONITORING series. This series describes research conducted to develop new or improved methods and instrumentation for the identification and quantification of environmental pollutants at the lowest conceivably significant concentrations. It also includes studies to determine the ambient concentrations of pollutants in the environment and/or the variance of pollutants as a function of time or meteorological factors.

This document is available to the public through the National Technical Information Service, Springfield, Virginia 22161.

TECHNICAL REPORT DATA
(Please read Instructions on the reverse before completing)

1. REPORT NO. EPA-600/4-79-052	2.
3. RECIPIENT'S ACCESSION NO. PB 80 169576	
4. TITLE AND SUBTITLE DISPERSION OF SULFUR DIOXIDE FROM THE CLINCH RIVER POWER PLANT A Wind-Tunnel Study	5. REPORT DATE September 1979 6. PERFORMING ORGANIZATION CODE
7. AUTHOR(S) Roger S. Thompson	8. PERFORMING ORGANIZATION REPORT NO. Fluid Modeling Report No. 7
9. PERFORMING ORGANIZATION NAME AND ADDRESS Environmental Sciences Research Laboratory Office of Research and Development U.S. Environmental Protection Agency Research Triangle Park, NC 27711	10. PROGRAM ELEMENT NO. 1AA603 AB-20 (FY-78) 11. CONTRACT/GRANT NO.
12. SPONSORING AGENCY NAME AND ADDRESS Environmental Sciences Research Laboratory -- RTP, NC Office of Research and Development U.S. Environmental Protection Agency Research Triangle Park, NC 27711	13. TYPE OF REPORT AND PERIOD COVERED in-house 6/77 - 12/78 14. SPONSORING AGENCY CODE EPA/600/09
15. SUPPLEMENTARY NOTES	

16. ABSTRACT

A wind-tunnel study of the transport and dispersion of sulfur dioxide from the Clinch River Power Plant in Virginia was performed for periods of neutral atmospheric conditions corresponding to two 1-hour periods for which field data were available. A 7-km x 21-km area of the quite rugged complex terrain surrounding the power plant was modeled at a scale of 1:1920 using a terraced construction. Exaggerated stack diameters were used in modeling the buoyant emissions from the plant's two stacks.

The most significant influences of terrain on the plume were found to be frequent downwashing and an angle of ~30° to the mean wind direction for the plume's initial direction. These phenomena were produced by the hills just upwind and downwind of the stacks. Ground-level concentrations measured at positions corresponding to field sampling sites compared well with field measured values. Comparisons of concentrations measured above the model surface with helicopter field measurements were not good, but the wind-tunnel measurements were shown to satisfy a conservation of mass requirement. The standard deviations of plume spread in the vertical and horizontal directions were measured for various downwind distances and compared to Pasquill-Gifford values for flat terrain. Ground-level concentrations under the plume centerline were compared to Gaussian plume model estimates, given the plume path and effective stack height determined experimentally.

17. KEY WORDS AND DOCUMENT ANALYSIS

a. DESCRIPTORS	b. IDENTIFIERS/OPEN ENDED TERMS	c. COSATI Field/Group
* Air pollution		13B
* Sulfur dioxide		07B
* Meteorology		04B
* Atmospheric diffusion		04A
Electric power plants		10B
* Wind tunnels		14B
Terrain models		

18. DISTRIBUTION STATEMENT RELEASE TO PUBLIC	19. SECURITY CLASS *(This Report)* UNCLASSIFIED 20. SECURITY CLASS *(This page)* UNCLASSIFIED	21. NO. OF PAGES 75 22. PRICE

EPA Form 2220-1 (9-73)

EPA-600/4-79-052
September 1979

DISPERSION OF SULFUR DIOXIDE FROM THE CLINCH RIVER POWER PLANT
A Wind-Tunnel Study

by

Roger S. Thompson
Meteorology and Assessment Division
Environmental Sciences Research Laboratory
Research Triangle Park, NC 27711

ENVIRONMENTAL SCIENCES RESEARCH LABORATORY
OFFICE OF RESEARCH AND DEVELOPMENT
U.S. ENVIRONMENTAL PROTECTION AGENCY
RESEARCH TRIANGLE PARK, NC 27711

DISCLAIMER

This report has been reviewed by the Environmental Sciences Research Laboratory, U.S. Environmental Protection Agency, and approved for publication. Mention of trade names or commercial products does not constitute endorsement or recommendation for use.

ABSTRACT

A wind-tunnel study of the transport and dispersion of sulfur dioxide from the Clinch River Power Plant in Virginia was performed for periods of neutral atmospheric conditions corresponding to two 1-hour periods for which field data were available. A 7-km x 21-km area of the quite rugged complex terrain surrounding the power plant was modeled at a scale of 1:1920 using a terraced construction. Exaggerated stack diameters were used in modeling the buoyant emissions from the plant's two stacks.

The most significant influences of terrain on the plume were found to be frequent downwashing and an angle of ~30° to the mean wind direction for the plume's initial direction. These phenomena were produced by the hills just upwind and downwind of the stacks. Ground-level concentrations measured at positions corresponding to field sampling sites compared well with field measured values. Comparisons of concentrations measured above the model surface with helicopter field measurements were not good, but the wind-tunnel measurements were shown to satisfy a conservation of mass requirement. The standard deviations of plume spread in the vertical and horizontal directions were measured for various downwind distances and compared to Pasquill-Gifford values for flat terrain. Ground-level concentrations under the plume centerline were compared to Gaussian plume model estimates, given the plume path and effective stack height determined experimentally.

CONTENTS

Abstract iii
Figures. vi
Tables ix
Symbols. x
Acknowledgements xi

1. Introduction. 1
2. Conclusions 3
3. Experimental Details and Procedures 7
   3.1 Field study. 7
   3.2 Selection of model scale and orientation 8
   3.3 Selection of periods to model. 9
   3.4 The Meteorological Wind Tunnel and modifications . . 12
   3.5 Model construction 14
   3.6 Similarity criteria ard constraints. 15
   3.7 Visualization and measurement techniques 21
4. Experimental Results and Discussion 23
   4.1 Wind-tunnel boundary layer 23
   4.2 Wind speed measurements. 23
   4.3 Plume visualization. 24
   4.4 Concentration measurements 25
   4.5 Plume spread 31

References 33

FIGURES

Number		Page
1	The EPA Meteorological Wind Tunnel without model or modifications in place.	34
2	Mean velocity measurements at Pibal site in the wind tunnel compared with field pibal measurements for July 24.	35
3	Mean velocity measurements at Pibal site in the wind tunnel compared with field pibal measurements for April 28.	35
4	Temperature (a) and wind direction (b) from field pibal releases.	36
5	Schematic of the model in the wind-tunnel test section showing the vortex generators, trip and roughness for boundary-layer generation, and the settling chamber.	37
6	Topographical map of the area modeled. Locations of field sites and wind-tunnel sampling positions are indicated.	38
7	The Clinch River terrain model in the wind tunnel. Vortex generators, sawtooth trip, and rows of roughness elements are upwind. Plant is in foreground.	39
8	Mean velocity measurements at various longitudinal positions in the wind tunnel for July 24, 1000-1100 EST conditions.	40
9	Mean velocity measurements at various longitudinal positions in the wind tunnel for April 28, 1800-1900 EST conditions.	40
10	Lateral homogeneity of the approaching boundary-layer flow. Mean velocity (a) and turbulence intensity (b) at a distance of 4 m from the upstream edge of the roughness. The velocity values are expressed in wind-tunnel units, u_{∞} = 1.0 m/s.	41
11	Mean velocity (a) and turbulence intensity (b) measured above Plant, Tower, and Pibal sites in the wind tunnel. Conditions modeled are July 24, 1000-1100 EST.	42
12	Mean velocity (a) and turbulence intensity (b) measured above Nash Ford, Munsey, and Lambert sites in the wind tunnel. Conditions modeled are July 24, 1000-1100 EST.	43

Number		Page
13	Mean velocity (a) and turbulence intensity (b) measured above Plant, Tower, and Pibal sites in the wind tunnel. Conditions modeled are April 28, 1800-1900 EST.	44
14	Mean velocity (a) and turbulence intensity (b) measured above Nash Ford, Munsey, and Lambert sites in the wind tunnel. Conditions modeled are April 28, 1800-1900 EST.	45
15	Photographs of the plume from one stack at the Clinch River Power Plant on July 24, 1977.	46
16	Photographs of the plume from one stack at the Clinch River Power Plant on July 24, 1977.	47
17	Flow visualization in the wind tunnel of July 24, 1000-1100 EST conditions.	48
18	Ground-level concentrations on the face of the hill just downwind of the plant for July 24, 1000-1100 EST conditions.	49
19	Ground-level concentrations at a distance of x = 0.64 km downwind of the stacks for July 24, 1000-1100 EST conditions.	50
20	Lateral ground-level concentration profile at a distance of x = 3.2 km downwind of the stacks for July 24, 1000-1100 EST conditions.	51
21	Lateral concentration profiles at a distance of x = 1.2 km downwind of the stacks for July 24, 1000-1100 EST conditions. Gaussian curve fits are drawn with the σ_y's specified.	52
22	Lateral concentration profiles at a distance of x = 2.3 km downwind of the stacks for July 24, 1000-1100 EST conditions. Gaussian curve fits are drawn with the σ_y's specified. Field helicopter data are also shown for a slightly later sampling period.	53
23	Lateral concentration profiles at a distance of x = 4.8 km downwind of the stacks for July 24, 1000-1100 EST conditions. Gaussian curve fits are drawn with the σ_y's specified.	54
24	Lateral concentration profiles at a distance of x = 8.2 km downwind of the stacks for July 24, 1000-1100 EST conditions. Gaussian curve fits are drawn with the σ_y's specified. Field helicopter data are also shown for a slightly later sampling period.	55

Number		Page
25	Ground-level concentrations under the plume centerline (Figure 6) for July 24, 1000-1100 EST conditions and April 28, 1800-1900 conditions.	56
26	Ground-level concentrations measured under plume centerline in wind tunnel compared with flat-terrain Gaussian model: $c = (Q/\pi\sigma_y\sigma_z u)\exp(-\frac{1}{2}(H/\sigma_z)^2)$, with σ_y and σ_z calculated for C stability.	57
27	Vertical concentration profile above Couch Cemetery for July 24 conditions, x = 1.65 km. Gaussian σ_z = 290 m.	58
28	Vertical concentration profile above Tower site for July 24 conditions, x = 3.2 km. Gaussian σ_z = 318 m.	58
29	Vertical concentration profile for July 24 conditions, x = 4.8 km, y = 0.4 km. Gaussian σ_z = 439 m.	59
30	Vertical concentration profile for July 24 conditions, x = 8.2 km, y = 0.4 km. Gaussian σ_z = 659 m.	59
31	Vertical concentration profile above Nash Ford site for July 24 conditions, x = 10.2 km. Gaussian σ_z = 857 m.	60
32	Vertical concentration profile for April 28 conditions, x = 1.2 km, y = 0.4 km. Gaussian σ_z = 192 m.	60
33	Vertical concentration profile for April 28 conditions, x = 2.3 km, y = 0.4 km. Gaussian σ_z = 187 m.	61
34	Vertical concentration profile above Tower site for April 28 conditions, x = 3.2 km. Gaussian σ_z = 225 m.	61
35	Wind-tunnel σ_y values for July 24 test conditions as compared with Pasquill-Gifford values.	62
36	Wind-tunnel σ_z values as compared with Pasquill-Gifford values.	62

TABLES

Number		Page
1	Summary of Field Conditions for the Clinch River Power Plant and Field Sampling Sites, July 24, 1977, 1000-1100 EST.	10
2	Summary of Field Conditions for the Clinch River Power Plant and Field Sampling Sites, April 28, 1977, 1800-1900 EST.	11

SYMBOLS

A	plume cross section area
c	concentration of pollutant
c_{max}	maximum concentration for a given profile
D	stack diameter
g	acceleration due to gravity
H_{eff}	effective source height including plume rise
L	length scale of model
L_B	buoyancy length parameter of plume
L_M	momentum length parameter of plume
N	number of layers used in approximating integral
Q	emission rate of pollutant from source
T_a	ambient air temperature
T_o	stack gas temperature
u	mean wind speed
u_s	mean wind speed at stack exit
$\sqrt{\overline{u'^2}}$	root mean square of wind speed fluctuations
w_o	stack gas exhaust speed
x	distance downwind from plant
y	distance perpendicular to wind direction
z	distance above local terrain surface
z_o	aerodynamic roughness length
Δz	increment of distance in the vertical
ρ	density
ρ_a	density of ambient air
ρ_o	density of stack gas
σ_y	standard deviation of lateral spread of plume
σ_z	standard deviation of vertical spread of plume

SUBSCRIPTS

$(\ )_1$	Stack 1
$(\ )_2$	Stack 2
$(\ )_f$	full-scale
$(\ )_m$	model scale
$(\ )_\infty$	free stream value

ACKNOWLEDGEMENTS

The author is grateful for the assistance of the entire staff of the Fluid Modeling Facility and to Mr. Len Marsh, in particular, who spent many hours collecting the wind-tunnel data. The cooperation of Geomet, Inc. employees who were contacted was greatly appreciated. Mr. David Bearden is to be commended for an excellent job of typing the final draft.

SECTION 1
INTRODUCTION

The effects of complex terrain on the transport and dispersion of pollutants released from point sources within such areas are not well understood. Adequate design (height and diameter) of smokestacks for power plants and factories located in hilly or mountainous regions must include an analysis of these effects. A 16-month field measurement program of dispersion from the Clinch River Power Plant was recently completed by Geomet, Inc. under contract 68-02-2260 with EPA. Data analysis and numerical modeling of the results are currently underway. This report describes an effort to complement and extend the data base of the field study by wind-tunnel modeling, makes direct comparisons of wind-tunnel and field measurements, and attempts to explain the physics and some of the anomalies of the flow over complex terrain.

A 1:1920 scale model of the terrain surrounding the power plant was constructed and installed in the EPA Meteorological Wind Tunnel. Dispersion of sulfur dioxide (SO_2) from the two stacks at the plant was studied for neutral atmospheric conditions. Wind speeds and pollutant concentrations were measured at various positions over the model. When possible, values measured in the model were compared with field measurements. Visualization of the plume was achieved through release of an oil fog from the model stacks. The emissions from the two stacks merged close to the plant to form one plume, hereafter referred to as "the plume."

Wind speed and concentration measurements at positions corresponding to fixed sampling sites of the field study compared favorably with the field measurements. The standard deviations of vertical and lateral plume spread were determined as a function of downwind distance.

The most significant influence of the complex terrain was a large initial spread of the plume near the power plant. A large hill upwind of the plant and extending above the stacks produced a highly turbulent flow that resulted in frequent downwashing of the plume. The local terrain then deflected the plume substantially from the mean flow direction until the plume rose above the terrain.

SECTION 2
CONCLUSIONS

A wind-tunnel study of dispersion of SO_2 from the stacks of a coal-fired power plant located in complex terrain was performed. A terraced model was constructed at a scale of 1:1920 and placed in the test section downwind of boundary-layer generation devices. Neutral atmospheric conditions with high wind speeds were modeled corresponding to two 1-hour periods for which field data were available. The conclusions of the study can be divided into three categories: comparisons of laboratory data and field data, remarks on dispersion over complex terrain, and general conclusions.

(1) Comparisons of the wind-tunnel measurements with field data were good. In specific:

(a) The wind fields matched quite well. Vertical profiles of wind speed determined from double theodolite-tracked gas-filled pilot balloons (pibals) released from a site near the plant were the goal for achievement of the boundary layer in the wind tunnel. A comparable profile was obtained over the pibal site in the model. Other available field data were wind speeds at 10 m for some of the fixed sampling sites. Agreement between these measurements in the wind tunnel and in the field was good.

(b) Qualitative smoke visualization of the plume near the stack showed terrain-induced downwash of the plume. Photographs of the actual plume were available and were quite similar to those of the model study.

(c) Ground-level concentrations compared quite well. For the July 24, 1000-1100 EST conditions, the Tower site SO_2 field concentration and wind-tunnel value were both 73 ppb. The Nash Ford site had 0 ppb in the field while the wind tunnel indicated a concentration below the field threshold of 1 ppb. For April 28, 1800-1900 EST, a Tower concentration of 4 ppb in the field compared to 95 ppb measured in the wind tunnel. However, the following hour, the field concentration was 21 ppb.

(d) The mobile sampling van was parked at two different sites on July 24. At one location, the van was positioned in the plume from the coal preparation plant and measured 15 ppb of SO_2. This source was not included in the wind-tunnel model and the power plant plume did not reach this location, resulting in a concentration of 0 ppb in the wind tunnel. At the other van location, the wind-tunnel concentration was 10 ppb while the van measured 35 ppb.

(e) Direct comparison of the "instantaneous" helicopter values with time-averaged values of the wind tunnel were not appropriate At a distance of 2.3 km from the plant, two helicopter traverses indicated a plume roughly 1/3 as wide and with higher peak concentrations than the corresponding wind-tunnel traverses. At a distance of 8.2 km from the plant, the available helicopter data were much more difficult to interpret and compare with model data. (At this time, field data have not been completely reduced or validated by Geomet and should be considered in that light.)

(2) The complex terrain influenced dispersion both initially at the release from the stacks and as the plume traveled downwind.

(a) The Clinch River Power Plant is located on an oxbow of the river. For the wind direction considered in this study, a ridge extended around this oxbow upwind of the plant. There was a hill just downwind of the plant. The ridge and hill were slightly higher than the power plant stacks. Neutral flow over the ridge produced a turbulent wake that resulted in frequent downwashing of the plume and greatly enhanced the initial plume spread. The plume was forced to follow a path up the valley at about 30° to the mean freestream wind direction. This resulted in a lateral offset of the plume of about 500 m at downwind distances of greater than 2 km.

(b) The rough surface of the complex terrain region resulted in more rapid vertical plume spread than would be obtained over flat terrain. Gaussian curve fits resulted in values for vertical standard deviation of concentration (σ_z) that were between Pasquill-Gifford values for B and C stability (Turner, 1970). The horizontal profiles were also fit to Gaussian formulas, and values for lateral standard deviation of concentration (σ_y) were compared to Pasquill-Gifford values. Near the source, σ_y resembled that of C stability; at a distance of 10 km, it resembled that of D stability.

(c) Given the actual plume path (Conclusion 2a), the maximum ground-level concentration under the plume centerline agreed

surprisingly well with predictions using a flat terrain Gaussian model for Pasquill-Gifford C stability. The effective stack height, a function of the wind speed (which could not be determined a priori), was found to be less than the true stack height for both periods modeled.

(3) Some general conclusions and observations concerning wind-tunnel modeling of such sources in complex terrain in wind tunnels can be stated.

(a) Modeling buoyant plumes at such reduced scales requires very low wind-tunnel airspeeds. Generating a suitable boundary layer in the test section of a wind tunnel can be done with vortex generators, a trip, and surface roughness. But much effort and care must be spent in obtaining a laterally homogeneous approach flow at these low speeds.

(b) Exaggeration of the stack diameter to allow higher wind-tunnel speeds than strict geometric modeling would dictate was found to be a practical and workable technique, based on plume visualization experiments.

SECTION 3
EXPERIMENTAL DETAILS AND PROCEDURES

3.1 Field Study

The Clinch River Power Plant is located in Carbo, Virginia, about 200 km west of Roanoke. The area surrounding the plant is quite rugged, with closely-spaced hills typically extending 180 m above the river. The river valley is bounded by ridges of mountains 300 to 400 m high oriented along a NE-SW direction. The valley is roughly 15 km wide. The power plant has two stacks 138 m in height with diameters of 4.75 and 3.81 m. The plant has three boilers, two of which exhaust to the larger stack (hereafter referred to as Stack 1). The 712 MW plant is operated by the Appalachian Power Company and burns local low-sulfur coal. There is only one other source of pollution, a coal preparation plant, producing significant SO_2 concentrations within the area of the study. This plant is located about 3.5 km northeast of the power plant and less than 1 km northwest of the nearest fixed monitoring station. With northwesterly winds, relatively high concentrations of SO_2 at this station were easily distinguished as coming from the coal preparation plant.

The field study monitored emission conditions at the power plant, local meteorology, and concentrations of pollutants at eight fixed stations and at additional locations with a helicopter and two mobile vans. The temperature and volumetric flow from each boiler were recorded on an hourly basis. The emitted concentrations of SO_2 were calculated for each of the boilers based upon sulfur content and emission factors for the coal being burned. For comparison, measurement of SO_2 in the exhaust of one

boiler was made on an hourly basis. Of the eight fixed sites, two recorded wind speed and direction at two levels each (10 and 30 m); the rest measured wind speed and direction at 10 m only. Sulfur dioxide was monitored at all eight sites. Nitrogen oxide and oxides of nitrogen were monitored at six stations; particulates were monitored for sulfate analysis at five. Averaging time for the fixed stations was 1 hour. The mobile vans measured sulfur dioxide, nitrogen oxide, nitrogen dioxide, oxides of nitrogen, and ozone. To determine the wind speeds and directions aloft, pibals were released regularly from an open field near the plant. Many had T-sondes (temperature sounders) attached to provide information on the local temperature gradient or atmospheric stability. The field study is described in detail by Koch et al. (1979).

3.2 Selection of Model Scale and Orientation

A model scale on the order of 1:2000 was necessary to include field sampling sites in the area to be modeled. At this scale, an area of about 8 km by 20 km could be fit into the test section of the Meteorological Wind Tunnel (Figure 1). The field sampling site nearest to the power plant was Tower, at a distance of 3.2 km. An exact scale of 1:1920 was chosen to facilitate construction of a terraced model using standard materials and maps as to be described in Section 3.5.

A wind direction of 238° was selected for two reasons: (1) This direction is along the river valley and aligns the large mountain ridges that bound the river valley with the wind-tunnel walls. These ridges would be beyond the area modeled for most wind directions, and choosing a direction other than 238° would have made it difficult to include the

effects of these ridges in the wind-tunnel flow. (2) For this direction, there were two fixed sampling sites nearly directly downwind of the plant. Two other sites were also included in the modeled area.

3.3 Selection of Periods to Model

Periods of the field study that exhibited neutral conditions with fairly high wind speeds (10 m/s or greater) and an upper-level wind direction of ~238° needed to be selected from the field data. The selections were based upon data from pibals with T-sondes attached that were released within a few hours of the periods considered for modeling. In addition, the sampling and monitoring equipment had to be operational during the period. It was also desirable to have a mobile van sampling and the helicopter flying through the plume to provide data on concentrations at additional locations.

During a 2-week intensive measurement program, most of the above conditions were satisfied. July 24, 1977, 1000 to 1100 EST was chosen as the 1-hour period to model. Table 1 lists the meteorological conditions, plant operating conditions, and measured concentrations. A period with a higher wind speed - April 28, 1977, 1900 to 2000 EST - was also modeled, but there were no helicopter or mobile van data for that period (see Table 2). Figures 2 through 4 illustrate the pibal velocity and temperature profiles for these periods. For April 28, the pibal was taken much earlier in the day than the study hour. However, wind records at Hockey and Tower show that the winds were of about the same speed and direction throughout the day. Therefore, the pibal was considered to be representative of the study period.

TABLE 1. SUMMARY OF FIELD CONDITIONS FOR THE CLINCH RIVER POWER PLANT AND FIELD SAMPLING SITES, JULY 24, 1977, 1000-1100 EST

Plant Data

Unit Number	Temperature (K)	Airflow (m^3/s)	Calculated SO_2 Emission (g/s)	Meas. SO_2 Emission (g/s)
1	389	175 (254)*	248	———
2	---Unit 2 down for repair---			———
3	386	182 (275)*	253	233.0 (353)*

Sampling Site Data

Site	Wind Speed At 10 m (m/s)	Wind Dir. At 10 m	Wind Speed At 30 m (m/s)	Wind Dir. At 30 m	SO_2 Conc. (ppb)
Tower†	---Missing data---				73
Munsey	1.6	231°	-	-	0
Nash Ford	2.6	227°	-	-	0
Lambert	---Site not operational---				
Hockey	5.0	197°	6.6	232°	0

* Numbers in parentheses are values adjusted by Geomet, Inc. after completion of this wind-tunnel study.

† Ambient temperature = 301 K at Tower site. SO_2 concentration at Tower site for 0900-1000 EST = 38 ppb and for 1100-1200 EST = 21 ppb.

TABLE 2. SUMMARY OF FIELD CONDITIONS FOR THE CLINCH RIVER POWER PLANT AND FIELD SAMPLING SITES, APRIL 28, 1977, 1800-1900 EST

Plant Data

Unit Number	Temperature (K)	Airflow (m^3/s)	Calculated SO_2 Emission (g/s)	Meas. SO_2 Emission (g/s)
1	397	225 (327)*	376	____
2	407	232 (358)*	392	____
3	395	230 (350)*	388	Missing

Sampling Site Data

Site	Wind Speed At 10 m (m/s)	Wind Dir. At 10 m	Wind Speed At 30 m (m/s)	Wind Dir. At 30 m	SO_2 Conc. (ppb)
Tower†	6.45	256°	7.94	244°	4
Munsey	1.06	278°	____	____	0
Nash Ford	3.38	243°	____	____	0
Hockey	8.15	215°	9.31	234°	0
Lambert	2.67	261°	____	____	0

* Numbers in parentheses are values adjusted by Geomet, Inc. after completion of this wind-tunnel study.

† Ambient temperature = 290 K at Tower site. SO_2 concentration at Tower site for 1700-1800 EST = 4 ppb and for 1900-2000 EST = 21 ppb.

The wind speed profiles of Figure 2 show the wind speed approaching a constant value at approximately z = 800 m. Figure 4b indicates the wind direction at this height to be within a few degrees of 238° for each of the pibals. By extending the logarithmic wind speed profiles of Figures 2 and 3 to u = 0, an aerodynamic roughness length for this terrain is seen to be on the order of 20 m. Points below z = 100 m should be ignored, since they fall below the typical nearby mountain height. Thompson (1978) found values on the order of 30 m in an earlier analysis of pibal data from this site for this wind direction. Thus, an 800-m-high logarithmic boundary layer with a z_o of 20 m and freestream wind direction of 238° was selected to approximate the field conditions for the study periods considered.

3.4 The Meteorological Wind Tunnel and Modifications

The EPA Meteorological Wind Tunnel (Figure 1) has a test section that is 3.7 m wide, 2.1 m high, and 18.3 m long and is an open-circuit tunnel suitable for modeling neutral atmospheric flows. The fan and a diffuser are located downstream of the test section in a sound-attenuating enclosure. At the entrance of the wind tunnel, a honeycomb and four screens straighten the flow and remove the large-scale turbulence. A contraction joins the entrance section to the test section. A more complete description of the tunnel may be found in Thompson and Snyder (1976) or Snyder (1979).

The wind tunnel was designed to operate at a maximum speed of 10 m/s. At the beginning of this study, operating the tunnel at speeds of 1 m/s or less resulted in unsteady flow patterns. The boundary-layer depth and velocity profile changed from run to run and sometimes during a given run. The

following arrangement of devices upstream of the test section produced a steady boundary-layer flow over the model: A settling chamber was constructed to shroud the entrance of the wind tunnel (Figure 5). The chamber, left open at the top, was 6.1 m wide, 3.66 m high, and 2.44 m deep (20 ft by 12 ft by 8 ft); that is, as wide as the wind-tunnel entrance and 85% as high. The chamber was installed to serve two purposes: (1) Air was drawn into the chamber from a given level in the room to avoid enhancement of the vertical room temperature stratification through the contraction. (2) Influence from air currents in the laboratory was minimized.

A section of Verticel (paper triangular cell honeycomb; cell length = 0.15 m and hydraulic diameter = 0.01 m) was installed at the exit of the contraction; that is, at the upstream end of the test section. The flow through the lower section of the honeycomb was found to vary slightly across the width of the test section. The variations were minimized by blocking the regions of high velocity with strips of paper tape. Two fiberglass screens (16 x 18 mesh) separated by 0.1 m were placed just downstream of this honeycomb to produce an additional pressure drop and help smooth any remaining velocity variations.

Figure 5 shows the arrangement of vortex-generating fins, sawtooth trip, and roughness blocks that was found to produce the desired boundary-layer velocity profile. As suggested by Counihan (1969), vortex-generating fins were used to initiate the boundary layer flow. The fins were 0.61 m high, 0.30 m in the flow direction, and 0.07 m wide at the rear of their base. They were spaced on 0.30 m centers across the span of the test section. A 0.14-m-high sawtooth trip with 0.04-m-high teeth cut on a

45° angle placed downwind of the vortex-generating fins was found to produce a more laterally homogeneous flow than the castellated barrier placed upwind used by Counihan. Staggered rows, 0.16 m on center, of 0.04-m x 0.04-m x 0.24-m blocks separated by 0.24 m within rows served as roughness elements over the next 5 m of the test section. To avoid an abrupt change at the upwind edge of the model, the height was increased for a few blocks just upwind of the portions of the model with larger mountains.

3.5 Model Construction

A terraced model was constructed from 0.0064-m (1/4-in) plywood sheets; each thickness of plywood corresponding to the 12.2-m elevation intervals of U.S. Geologic Survey (USGS) topographic maps to give a model scale of 1:1920. At this scale, a model of a 7-km x 21-km area of the Clinch River Valley was constructed to occupy a 3.66-m-wide by 11-m-long portion of the Meteorological Wind Tunnel test section. The terrain model was constructed by Model Display Studio, Inc. of Raleigh, N.C. using a technique developed by the Calspan Corporation (Ludwig and Skinner, 1976). As shown in Figure 6, the modeled area included the power plant and four of the field sampling sites. The area was laid out on a composite map using the USGS maps (1:24000 scale, divided into sections representing 1.22-m (4-ft) squares of the model). Each section was photographed and two 1.22-m-square prints were made of each section. These prints were glued to 1.22-m-square sheets of 0.0064-m-thick plywood. For each pair of sheets corresponding to a given area, every other contour line on one sheet was cut with a saber saw; the same was done to the other sheet for the inter-

mediate contour lines. These pieces were then stacked (by alternating pieces from the two sheets) and glued and nailed together to form the sections of the terraced model (Figure 7). Each section was mounted on a firm base of 0.0127-m (1/2-in) plywood and built up to the proper level to match the neighboring sections in elevation. The squares were painted with a light coat of green paint without covering the printing on the maps. The sections of the model were fastened to the floor of the wind-tunnel test section with wood screws in each corner. All joints were filled with architectural putty.

3.6 Similarity Criteria and Constraints

In modeling dispersion from stacks, the momentum and buoyancy of the plume must be properly scaled. It is also desirable to maintain the highest possible Reynolds number value based on stack diameter and exit velocity. If the Reynolds number is too low, the plume will be laminar and the entrainment mechanism of the model will not resemble that in the field.

Exaggeration of the diameter of the model stacks (that is, making them larger in the model than the geometric scale dictates) helps to increase the Reynolds numbers of the stacks and also increases the operating speed of the tunnel (Liu and Lin 1976). Too severe of an exaggeration, however, reduces the effluent-speed-to-wind-speed ratio to a point where stack-induced downwash of the plume occurs. An exaggeration of about 2.9 was used for the stacks in this study. The exaggeration factor was determined by selecting sizes of available tubing that would provide both stacks with nearly the same exaggeration while keeping the ratios of exit velocity

to crosswind speed greater than 1.0. The 4.75-m-diameter stack was modeled with a 0.0072-m-diameter stack, and the 3.81-m-diameter stack was modeled with a 0.0056-m-diameter stack. To help ensure turbulence of the plume at the stack exit, a trip in the form of an orifice was installed in each stack (Liu and Lin 1976). For each stack, the diameter of the opening in the orifice was one-half the inside diameter of the stack and the orifice was placed 10 stack diameters from the stack exit.

For the model effluent, a buoyant gas that could serve as a tracer and be measured by the flame ionization detector was needed. Using a single gas provided more accurate control of the effluent rate than mixing gases to balance densities and tracer concentrations. Thus, pure methane (ρ/ρ_a = 0.57) was selected as the model effluent. For flow visualization experiments, air and helium were mixed to obtain an effluent with the same density as methane.

Proper modeling of the buoyant release using an exaggerated stack diameter was accomplished by adjusting the effluent conditions to scale the buoyancy length and momentum length of the plume according to the geometric length scale of the model (1:1920). Briggs (1975) defines these characteristic lengths as:

$$L_B = \text{buoyancy length} = \frac{g}{4} \frac{(To-Ta)}{To} \frac{w_o \; D^2}{u_s^3}$$

$$L_M = \text{momentum length} = \frac{1}{2}(T_a/T_o)^{\frac{1}{2}} \frac{w_o \; D}{u_s}$$

If we use the subscripts f for field and m for wind tunnel, the scaling criteria is stated as:

$$L_{Bm} = L_{Bf} \ / \ 1920$$

$$L_{Mm} = L_{Mf} \ / \ 1920$$

Also, where gases of different density are used to model field temperature differences, we substitute $(\rho_a - \rho_o)/\rho_a$ for $(T_o - T_a)/T_o$ and (ρ_o/ρ_a) for (T_a/T_o) in the above formulas (ρ_o and ρ_a are the effluent and ambient gas densities).

Inserting known values of the parameters from the field and model enables solving for each stack's effluent rate and for the wind-tunnel speed. Since a field measurement of the wind speed at the top of the stacks was not made, the wind-tunnel value is used to estimate the wind speed at the stack exit in the field. As discussed in Section 4, wind-tunnel velocity measurements indicated the mean wind speed at the stack exits to be about 0.47 times the freestream tunnel speed. The mean speed aloft was 9 m/s for the July 24, 1977 study period. Therefore, $(u_s)_f = 0.47 \times 9 \text{ m/s} = 4.2 \text{ m/s}$.

For Stack 1 (the larger-diameter stack), the exit velocity is computed from the data in Table 1 to be $(w_o)_f = 9.88$ m/s. Substituting these known values into the momentum length scaling requirement results in

$$(w_o)_m \ / \ (u_s)_m = 0.94$$

and, for the buoyancy length requirement,

$$(w_o)_m \ / (u_s)^3_m = 15.9 \ s^2/m^2$$

Solving these two equations for $(w_o)_m$ and $(u_s)_m$ yields

$$(w_o)_m = 0.23 \text{ m/s}$$

$$(u_s)_m = 0.24 \text{ m/s}$$

Performing the same calculations for Stack 2 results in

$$(w_o)m = 0.38 \text{ m/s}$$

$$(u_s)m = 0.24 \text{ m/s}$$

The freestream wind speed for the wind tunnel is then computed to be

$$(u_\infty)m = (0.24 \text{ m/s})/0.47 = 0.5 \text{ m/s}$$

and effluent rates for the two stacks are

$$(Q_1)_m = (w_{o1})_m(\pi D_1^2/4) = 580 \text{ cm}^3/\text{min}$$

$$(Q_2)m = (w_{o2})_m(\pi D_2^2/4) = 560 \text{ cm}^3/\text{min}$$

Computations for the April 28, 1977 study period result in the following conditions:

$$(u_\infty)_m = 1.0 \text{ m/s}$$

$$(w_{o1})_m = 0.49 \text{ m/s}$$

$$(w_{o2})_m = 0.42 \text{ m/s}$$

$$(Q_1)_m = 1260 \text{ cm}^3/\text{min}$$

$$(Q_2)_m = 630 \text{ cm}^3/\text{min}$$

After this wind-tunnel study was completed using stack airflow rates from quarterly reports of the field study, Geomet, Inc. revised their method of computation, resulting in adjusted airflow rates of about 40

to 50 percent higher. The airflow rates enter the plume scaling calculations as a linear effect on both L_B and L_M; thus, these values should have been 40 to 50 percent larger in the wind-tunnel study for exact modeling. However, the highly turbulent flow in the vicinity of the stacks produced a strong terrain-induced downwash that resulted in a large initial spreading of the plume. A 50 percent increase in L_B and L_M would probably not produce an observable difference in the plume shape or a significant difference in concentration.

For multiple sources with exaggerated stack diameters and stack exit velocities, the proportion of tracer gas that should be released from each of the stacks to enable simple relation of the wind-tunnel measurements to the fullscale values is not immediately obvious. It is shown below that the ratio of mass fluxes of tracer for the model stacks must be the same as for the pollutant mass fluxes for the fullscale stacks.

The concentration (in mass per unit volume) of a pollutant c at a position in the plume is proportional to the effluent rate (in mass per unit time) of the source Q and inversely proportional to the mean wind speed u and the plume cross-sectional area A. That is, $c \propto Q/uA$. Consider, both for the fullscale and for the model, a position downwind of two stacks where concentrations from each are present:

Fullscale Stack 1: $c_{f1} \propto Q_{f1}/u_{f1}A_{f1}$

Model Stack 1: $c_{m1} \propto Q_{m1}/u_{m1}A_{m1}$

Fullscale Stack 2: $c_{f2} \propto Q_{f2}/u_{f2}A_{f2}$

Model Stack 2: $c_{m2} \propto Q_{m2}/u_{m2}A_{m2}$

or

$$c_{f1} = \frac{Q_{f1}u_m A_{m1}}{Q_{m1}u_f A_{f1}} c_{m1}$$

$$c_{f2} = \frac{Q_{f2}u_m A_{m2}}{Q_{m2}u_f A_{f2}} c_{m2}$$

What we desire is a relation between the fullscale concentration, $c_f = c_{f1} + c_{f2}$, and the model concentration, $c_m = c_{m1} + c_{m2}$. Assuming the same plume shape and spread in the model and field,

$$A_{m1}/A_{f1} = A_{m2}/A_{f2} = L^2$$

where L is the geometric length scale of the model.

$$c_f = c_{f1} + c_{f2} = \frac{Q_{f1}}{Q_{m1}} \frac{u_m}{u_f} \frac{A_{m1}}{A_{f1}} c_{m1} + \frac{Q_{f2}}{Q_{m1}} \frac{u_m}{u_f} \frac{A_{m2}}{A_{f2}} c_{m2}$$

$$= \frac{Q_f}{Q_m} \frac{u_m}{u_f} \frac{L^2}{} (c_{m1} + c_{m2}) = \frac{Q_f}{Q_m} \frac{u_m}{u_f} \frac{L^2}{} c_m$$

if we set $Q_{f1}/Q_{m1} = Q_{f2}/Q_{m2} = Q_f/Q_m$. That is, if the ratio of the mass flux of the tracer for the model stacks is equal to the ratio of the fluxes of the pollutants for the fullscale stacks, the model concentrations can be used to calculate fullscale values according to:

$$c_f = (Q_f/Q_m)\ (u_m/u_f)\ (L^2)\ c_m\ .$$

Since there were only two stacks that were emitting roughly the same concentrations of SO_2 and the model diameters were scaled at nearly the same exaggeration, emitting pure methane as the tracer from both stacks

resulted in the correct proportion of tracer in each stack. Because of this, concentrations measured in the model were easily converted to field values. Thus, for the July 24, 1977 study period:

$$c_f = \frac{(501 \text{ g } SO_2/s)\ (0.5 \text{ m/s})\ (\frac{60s}{min})\ (\frac{1 \times 10^{-6} \text{ m}^3 SO_2}{2.93 \times 10^{-3} \text{ g } SO_2})}{(1.14 \times 10^{-3} \text{ m}^3 CH_4/min)\ (9 \text{ m/s})\ (1920)^2}\ c_m$$

or $c_f = 1.36 \times 10^{-4}\ c_m$, where concentrations are now expressed on a volume/volume basis. Similarly, for the April 28, 1977 period, $c_f = 1.7 \times 10^{-4}\ c_m$.

Correct modeling of atmospheric flow and dispersion in wind tunnels requires satisfying many other similarity criteria. Standard procedures were followed for meeting the imposed conditions.

3.7 Visualization and Measurement Techniques

Flow visualization of the plume was performed using a paraffin-oil smoke-generation apparatus. Air and helium were mixed in the proper ratio to produce the desired density of effluent and correct total flow rate for both stacks. The flow rates of air and helium were monitored with Meriam Laminar Flow Elements. Paraffin oil was vaporized in an in-line canister by pumping the air-helium mixture from the canister and returning it through an aspirating nozzle that drew oil from the bottom of the canister and sprayed it onto the tip of a hot soldering iron. Valves on the lines to the stacks were adjusted to divide the flow between the stacks in the correct proportion. The flow rate to each stack was checked with a bubble meter and stopwatch. Photographs of the smoke patterns were taken with a 35-mm camera using black and white ASA 400 film. A shutter speed of 1/30 s and an aperture of f/16 were used.

Velocity and turbulence intensity measurements were made with a Thermo-Systems hot-film anemometer. The anemometer (Model 1053B) and Model 1057 signal conditioner controlled a Model 1212 single cylindrical probe. The analog output of this system was digitized, processed, and stored on disk by a Digital Equipment Corporation PDP-11/40 minicomputer. For routine velocity measurements, a 120-s sampling period and a rate of 250 samples/s were used. When raw data were to be stored for later spectral analysis, sampling rates ranged as high as 1000 samples/s for 120 s. Calibration was achieved by positioning the probe in the freestream flow above the model. Smoke puffs were released into the flow and timed over a fixed distance to determine airspeed at low speeds; at high speeds, a pitot tube and manometer were used to obtain six calibration speeds.

A tank of 99% pure methane served as the supply of tracer gas for concentration measurements. This tank fed two lines, one to each stack, each with a metering valve and a Model 50MK10-2 Meriam Laminar Flow Element to control the desired efflux rate for each stack.

Mean methane concentrations were measured at selected points over the model by use of a Beckman 400 Hydrocarbon Analyzer. A small pump drew a continuous sample through a 0.002-m-diameter probe and fed it directly to the analyzer. The minicomputer was again used to process and store the data. Since the response of the hydrocarbon analyzer is only 0.5 s and (therefore) only mean concentrations can be obtained, a sampling rate of 50 samples/s for 120 s was used.

SECTION 4

EXPERIMENTAL RESULTS AND DISCUSSION

With the exception of the discussion of the approach boundary layer, all results are presented in field units. That is, concentrations are in parts per billion SO_2 that would be observed in the field, distances are fullscale, etc. The coordinate system has its origin at the power plant, x is measured directly downwind (azimuth = 58°), y is to the WNW (azimuth = 328°), and z is the vertical distance from the local surface. "Elevations" are from mean sea level.

4.1 Wind-Tunnel Boundary Layer

The desired characteristics of the boundary layer over the model were based on the field pibal measurements. The pibal was released near the plant with the terrain upwind of the release site typical of the modeled area. That is, there were no extremely large hills or regions of relatively smooth terrain just upwind of the field pibal site. Roughness elements placed upwind of the terrain model were selected to produce a scaled z_o of 1/1920th of the field value. The wind-tunnel measurements of the wind speed profile at the pibal site are shown in Figures 2 and 3 for comparison with the field data. Figures 8 and 9 illustrate variations in the mean wind profile along the model for the two study periods. Good lateral homogeneity was achieved in the approach boundary layer (Figure 10) using the arrangement of devices described earlier.

4.2 Wind Speed Measurements

Mean velocities and turbulence intensities for July 24, 1000-1100 EST are presented in Figures 11 and 12. Figures 13 and 14 present these

parameters for April 28, 1800-1900 EST. The mean velocity at the height of the stacks (138 m) over the plant site was 4.6 m/s for July 24 (Figure 11) and 9.3 m/s for April 28 (Figure 13). The ratios of these values to freestream speed are 4.6/9.0 = 0.51 and 9.3/20 = 0.47. The value of 0.47 was available at the time of emission conditions design and was used in the analysis presented in Section 3.6.

With the exception of Munsey and Lambert (Figure 12a), mean velocity profiles were quite similar for all sites. Munsey and Lambert exhibited higher velocities than the other locations for July 24 conditions. These sites were near the wind-tunnel wall. The boundary layer on the wall at the low wind-tunnel speed (0.5 m/s) could have produced a small region of higher velocity above these sites to compensate for the velocity deficit of the wall boundary layer.

Available field measurements of wind speed are also shown in Figures 12 and 13. All measurements were made at a height of 10 m, which is near the surface where the speed increases quite rapidly with height. However, the field measurements agreed quite well with the wind-tunnel values.

4.3 Plume Visualization

During the intensive field measurement portion of the Geomet, Inc. study, photographs of the power plant plume were fortunately made possible through reduction of the electrostatic precipitators for one stack. Figures 15 and 16 present two series of photographs taken at 2-min intervals. The erratic nature of the plume path is noteworthy. In Figure 15b, the plume is rising nearly vertically; in Figures 15a and 15d, 2 min before and 4 min after, the plume is leaving the stack nearly horizontally.

The extent of the downwash can be seen in Figure 16a where the plume is nearly touching the ground at the base of the stack. Similar plume patterns were observed in the smoke visualization experiments of the wind-tunnel study (Figure 17). Notice the downwash in Figure 17a and the similarity to Figure 16a.

The power plant is located just downwind of a large hill extending 120-150 m above the valley that wraps around the plant from west to north (see Figure 6). There is also a large hill extending 160 m above the valley downwind of the plant. This forms a channel that deflects the plume toward the north for the wind direction studied. Figure 17d is a top-view photograph of the wind-tunnel plume that demonstrates the amount of plume deflection. Concentration measurements to be presented later confirm this plume path.

4.4 Concentration Measurements

Tracer concentrations were measured at various positions on the ground and aloft. Attempts were made to reproduce field measurements when possible; thus, more measurements were made for the July 24 period than for the April 28 period.

In spite of frequent downwashing of the plume, ground-level concentrations measured near the base of the stack for July 24 conditions were negligible. Measurements on the face of the hill just downwind of the stack (see Figure 6) were quite low, with a value of 13 ppb occurring on the hill top (Figure 18). This was due primarily to deflection of the plume around this hill to the north. A lateral ground-level traverse (Figure 19) across the plume over this hill top, $x = 0.64$ km, shows a maximum concentration of 122 ppb offset a distance of $y = 360$ m. That

is, the maximum ground-level concentration occurred 30° from the freestream wind direction. At a distance of x = 3.2 km, the maximum ground-level concentration was 82 ppb and the offset was ~500 m (Figure 20).

Lateral traverses at constant elevation were made at downwind distances of x = 1.2, 2.3, 4.8, and 8.2 km (Figures 21-24, respectively) for July 24, 1000-1100 EST. Curves of the form $c = c_{max}\exp(-0.5(y/\sigma_y)^2)$ were fit to each traverse to determine the standard deviation, σ_y, of the lateral plume spread. The lateral shift of the plume centerline increased to 500 m at a distance of x = 2.3 km and remained at that approximate value for farther downwind distances.

Helicopter field data were available for x = 2.3 km and 8.2 km and are shown for comparison in Figures 22 and 24. The helicopter data were raw data from a magnetic tape supplied by Geomet, Inc. Geomet had not completed analysis and validity-checking of this data.

Direct comparison of the wind-tunnel and helicopter data was difficult partly because of the difference in sampling times. The helicopter data were nearly instantaneous, since it took only about 2 minutes to fly through the plume; the wind-tunnel results, in contrast, were time-averaged values. Also, the helicopter data for x = 8.2 km were obtained for a later period in the day; emission rates and meteorological conditions were quite similar to those for the modeled period, however.

The helicopter profile at x = 2.3 km and elevation of 1158 m showed a high background level. This was most likely due to a problem with the sampling equipment; since only raw data were available, however, the values were plotted uncorrected (Figure 22). A background level of 45 ppb was

removed from this profile for comparison with the wind-tunnel data. At an elevation of 1158 m, the peak field SO_2 concentration minus background was 50 ppb and the peak wind-tunnel concentration was 40 ppb. At an elevation of 975 m, the peak field concentration was 65 ppb and the peak wind-tunnel concentration was 50 ppb. The helicopter sampled a plume about one-third as wide as the wind-tunnel plume and with a somewhat higher maximum concentration.

At a downwind distance of x = 8.2 km (Figure 24), the helicopter data were more difficult to compare with the wind-tunnel data. The helicopter profiles showed multiple peaks, and at the higher elevations the lateral profiles were much wider than those in the wind tunnel. The maximum concentration for each elevation measured by helicopter was about double the concentration measured in the wind tunnel.

As a check on the lateral concentration profiles at this downwind distance, a conservation of mass calculation can be made for the wind-tunnel data. The mass continuity requirement is stated as

$$Q = \int_0^{\infty} \int_{-\infty}^{\infty} u\, c\, dy\, dz$$

That is, the rate of mass leaving the source is equal to the rate of mass crossing a plane downwind of the source. A Gaussian distribution, with σ_y = a constant independent of z, is assumed to give

$$c = c_{max}(z)\ \exp(-\tfrac{1}{2}(y/\sigma_y)^2)$$

This is integrated to give

$$Q = \sqrt{2\pi}\ \sigma_y \int_0^\infty c_{max}\,(z)\ u\,(z)\ dz$$

which is approximated by

$$Q = \sqrt{2\pi}\ \sigma_y \sum_{i=1}^{N} c_{max}\,(z_i)\ u\,(z_i)\ (\Delta z)_i$$

This calculation was performed for the July 24, x = 8.2 km wind-tunnel data using N = 6 layers in the vertical. A calculated Q of 470 g/s SO_2 was obtained for comparison with the actual source rate of 501 g/s SO_2. Thus, the wind-tunnel data satisfied the mass conservation requirement to within ~6% using this rough approximation technique. The helicopter data, which showed much higher concentrations and a wider plume (and hence more SO_2 passing this plane) can be questioned.

Ground-level concentrations were measured under the plume centerline as determined from the lateral ground-level and elevated traverses (Figure 6). Figure 25 shows measurements for both modeled periods and the terrain elevation. For the first 1.4 km, the plume followed the local valley (elevation = 460 m); then the path went up over Sinkhole Valley (elevation = 600 m). For both July 24 and April 28, the maximum ground-level concentration occurred on the local river valley before the plume encountered the valley wall. This suggests that the plume rose to accommodate the increasing terrain height rather than colliding with the terrain. These data are plotted on logarithmic axes in Figure 26. Also plotted are ground-level concentrations to be expected over flat terrain with

a uniform wind field. As described by Turner (1970), the Gaussian model for this case is $c = (Q/\pi\sigma_y \sigma_z u)\exp(-0.5(H_{eff}/\sigma_z)^2$. The freestream wind speed, u, was used with σ_y and σ_z for Pasquill-Gifford atmospheric stability C (slightly unstable). Had Pasquill-Gifford σ_y and σ_z for B or D stability been used, the distance to the maximum ground-level concentration would not match the wind-tunnel result. Previous wind-tunnel experiments (Huber et al. 1979) have shown boundary layers in the EPA Meteorological Wind Tunnel to exhibit plume spreads characteristic of C stability in the vertical and D stability in the lateral directions. For July 24 conditions (Figure 26a), an effective stack height of ~100 m resulted in a good fit to the data. For April 28 (Figure 26b), the effective height was found to be 75 m. As a result of downwashing of the plume, concentrations near the plant were much higher than the Gaussian model estimates. It should be emphasized that state of the art techniques do not provide for a priori estimation of H_{eff} or the plume path for this complex terrain situation. The comparison here was made primarily to examine the nature of the reduction of ground-level concentration with distance from the source for the wind-tunnel study, and not to suggest that Gaussian plume theory is necessarily a good predictive tool.

On July 24, the mobile van sampled SO_2 at two locations. From 0919 to 1030 EST, the van was located on a bearing of 25° at a distance of 4 km from the plant. During that time, SO_2 concentrations were 13-16 ppb. On the model, this position corresponds to x = 3.2 km, y = 2.0 km, just beyond the lateral extent of the lateral wind-tunnel profile measured at x = 3.2 km (Figure 20). Therefore, the comparable wind-tunnel concen-

tration was C ppb. One possible reason for the higher level observed in the field could be that this sampling position was 0.76 km directly downwind of the coal preparation plant mentioned (the only other significant source in the area).

From 1249 to 1348 EST, the van was located on a bearing of 57° at a distance of 11.2 km from the plant. SO_2 levels of 33-37 ppb were measured. This position was near the plume centerline, for which Figures 25 and 26a show concentrations. Concentrations in the wind tunnel were measured out to a distance of 8 km. Extrapolating to a distance of 11.2 km yielded a concentration of ~10 ppb.

Vertical traverses were made at field sampling sites, at downwind distances of lateral profiles, and at some intermediate positions. Figures 27-31 are for July 24, 1000-1100 EST conditions for downwind distances of x = 1.65, 3.2, 4.8, and 10.2 km, respectively. Figures 32-34 are for April 28, 1800-1900 EST conditions and distances of x = 1.2, 2.3, and 3.2 km. To determine a parameter describing the vertical spread of the plume, a reflected Gaussian plume shape was assumed:

$$c = c_{max}[\exp(-0.5((z-H_{eff})/\sigma_z)^2) + \exp(-0.5((z+H_{eff})/\sigma_z)^2)]$$

(see Turner 1970). Effective stack heights of 100 m and 75 m were used for July 24 and April 28, respectively. A best fit routine was used to compute the standard deviation, σ_z. Field data for the fixed sampling sites are included on Figures 28, 31, and 34. Good agreement was obtained for Tower site on July 24 (Figure 28). For the 1000-1100 EST period modeled, the wind-tunnel concentration was 73 ppb, exactly the value recorded in

the field. For the preceding and following 1-hour periods, the field concentrations were somewhat less, at 38 and 21 ppb. For this same period, wind-tunnel values at the Nash Ford site (Figure 31) were below the field threshold value of 1 ppb. The field concentrations were below threshold for the preceding and following periods as well. There was less agreement between field and wind-tunnel values for the April 28 conditions (Figure 34). In the wind tunnel, a value of 95 ppb was observed; in the field, only 4 ppb was detected for the modeled period and preceding hour and 21 ppb was measured for the following hour. The meteorological conditions were not as well defined for the April 28 model period as for July 24. The April 28 pibal was released much earlier in the day than the period modeled. An error in plume direction could have caused the wind-tunnel concentration to fall below the field value.

4.5 Plume Spread

The standard deviation of lateral plume spread (σ_y) and vertical plume spread (σ_z) as determined above can be compared directly with those of Pasquill-Gifford (Turner 1970) for flat terrain. The σ_y values for the July 24 period are shown in Figure 35. Near the source, σ_y was larger than for C stability; beyond x = 3 km, σ_y was less than for C stability. The downwind distance was measured from the stack; no virtual source position was attempted to compensate for the initial plume spread produced by the turbulent wake of the ridge just upwind of the stacks. The σ_y values determined for both of the modeled periods were larger than for Pasquill-Gifford C stability values. It is interesting to note that σ_z remains essentially constant at x = 1.65 and 3.2 km for July 24 and at 1.2 and

2.3 km for April 28. This was approximately where the plume had to climb above the river valley wall and the local surface elevation increased by about 140 m. This increase in terrain height produced a converging flow. Thus the vertical spread of the plume was severely limited to the extent that the increase in terrain height just offset any vertical growth of the plume.

REFERENCES

Briggs, G.A., 1975: Plume Rise Predictions, ATDL No. 75/15, Environmental Research Laboratory, National Oceanic and Atmospheric Administration, Oak Ridge, TN. 46 pp.

Counihan, J., 1969: An Improved Method of Simulating an Atmospheric Boundary Layer in a Wind Tunnel, Atmospheric Environment, 3, 197-214.

Huber, A.H., W.H. Snyder, R.S. Thompson and R.E. Lawson, 1979 (in press), The Effects of a Squat Building on Short Stack Effluents, Environmental Monitoring Series Report, U.S. Environmental Protection Agency, Research Triangle Park, NC.

Koch, R.C., W.G. Biggs, D. Cover, H. Rector, P.F. Stenberg, and K.E. Pickering, 1979: Power Plant Stack Plumes in Complex Terrain - Description of an Aerometric Field Study, EPA-600/7-79-010a, U.S. Environmental Protection Agency, Research Triangle Park, NC.

Liu, H.T. and J.T. Lin, 1976: Plume Dispersion in Stably Stratified Flows over Complex Terrain; Phase 2, EPA-600/4-76-022, U.S. Environmental Protection Agency, Research Triangle Park, NC.

Ludwig, G.R. and G.T. Skinner, 1976: Wind Tunnel Modeling Study of the Dispersion of Sulfur Dioxide in Southern Allegheny County, Pennsylvania, EPA 903/9-75-019, U.S. Environmental Protection Agency, Philadelphia, PA.

Snyder, W.H., 1972: Similarity Criteria for the Application of Fluid Models to the Study of Air Pollution Meteorology, Boundary Layer Meteorology, 3, 113-134.

Snyder, W.H., 1979: The EPA Meteorological Wind Tunnel - Its Design, Construction and Operating Characteristics, U.S. Environmental Protection Agency, Research Triangle Park, NC, (cleared for publication as EPA report).

Thompson, R.S. and W.H. Snyder, 1976: EPA Fluid Modeling Facility, in EPA 600/9-76-016, Proceedings of the Conference on Environmental Modeling and Simulation, U.S. Environmental Protection Agency, Washington, DC.

Thompson, R.S., 1978: Note on the Aerodynamic Roughness Length for Complex Terrain, J. Appl. Meteor., 17, 1402-1403.

Turner, D.B., 1970: Workbook of Atmospheric Dispersion Estimates, AP-26, Office of Air Programs, U.S. Environmental Protection Agency, Research Triangle Park, NC.

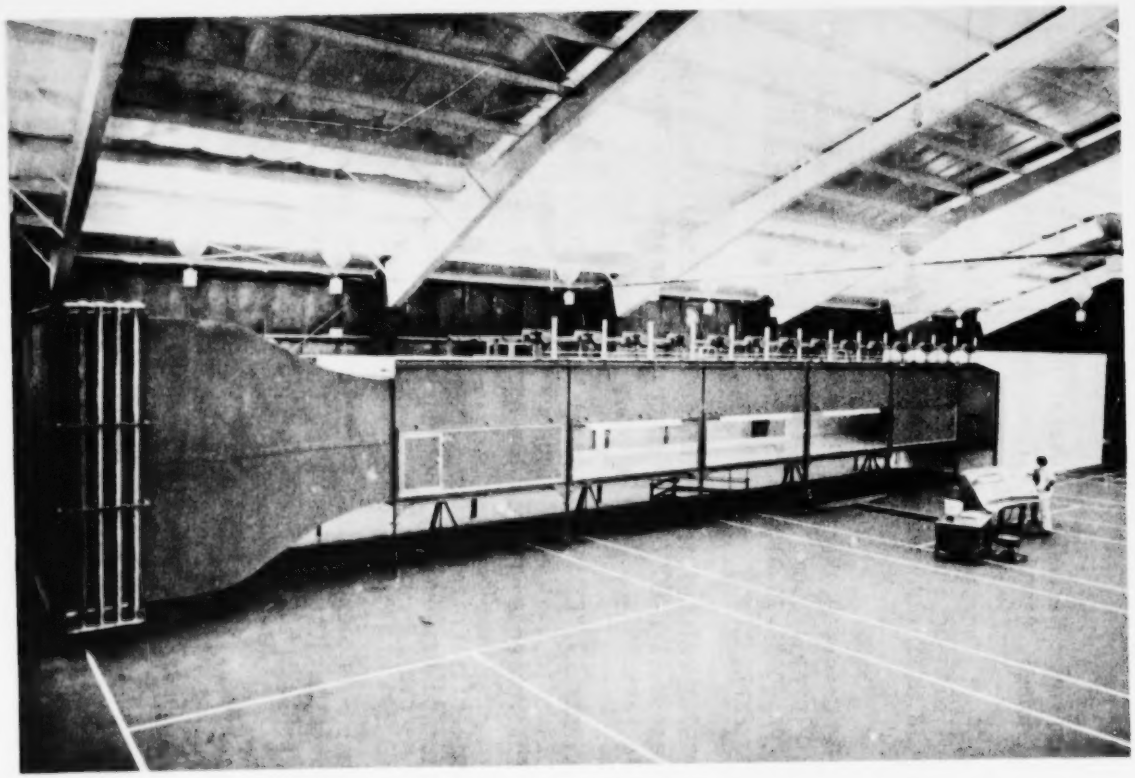

Figure 1. The EPA Meteorological Wind Tunnel without model or modifications in place.

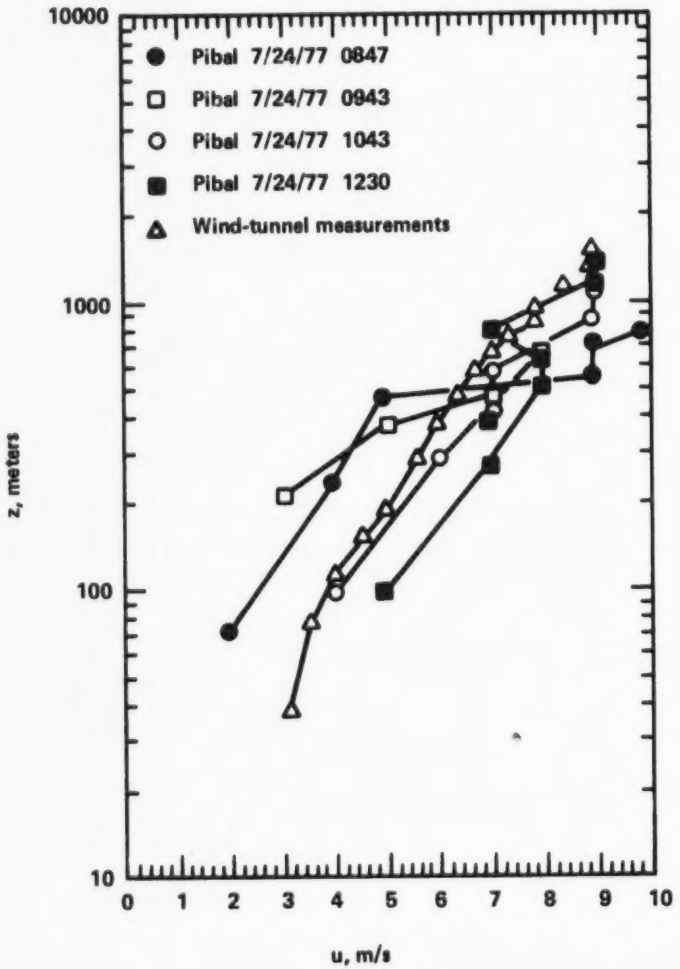

Figure 2. Mean velocity measurements at Pibal site in the wind tunnel compared with field pibal measurements for July 24.

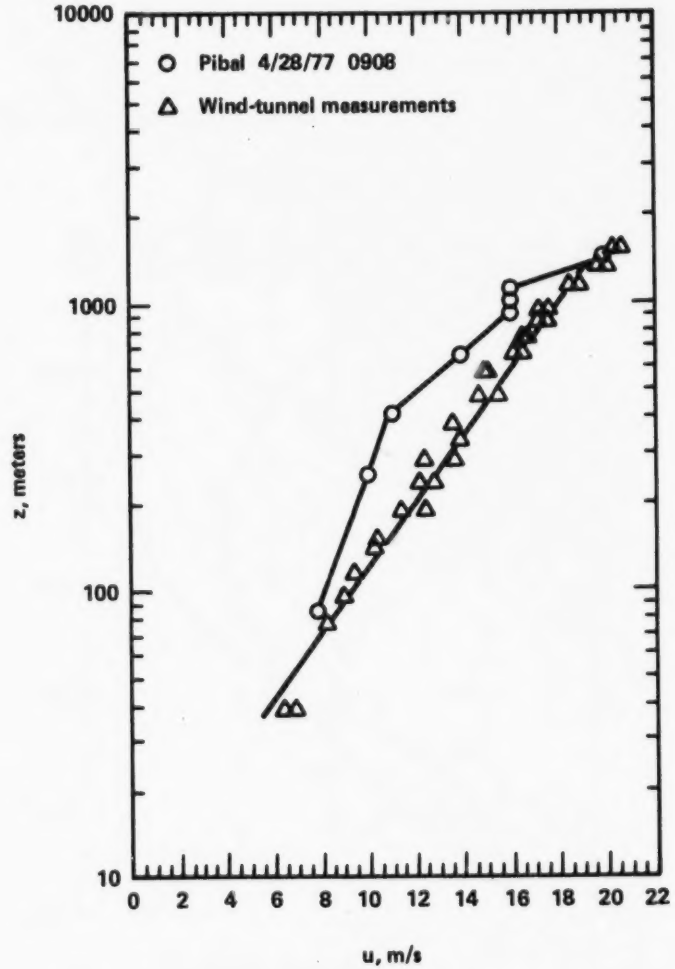

Figure 3. Mean velocity measurements at Pibal site in the wind tunnel compared with field pibal measurements for April 28.

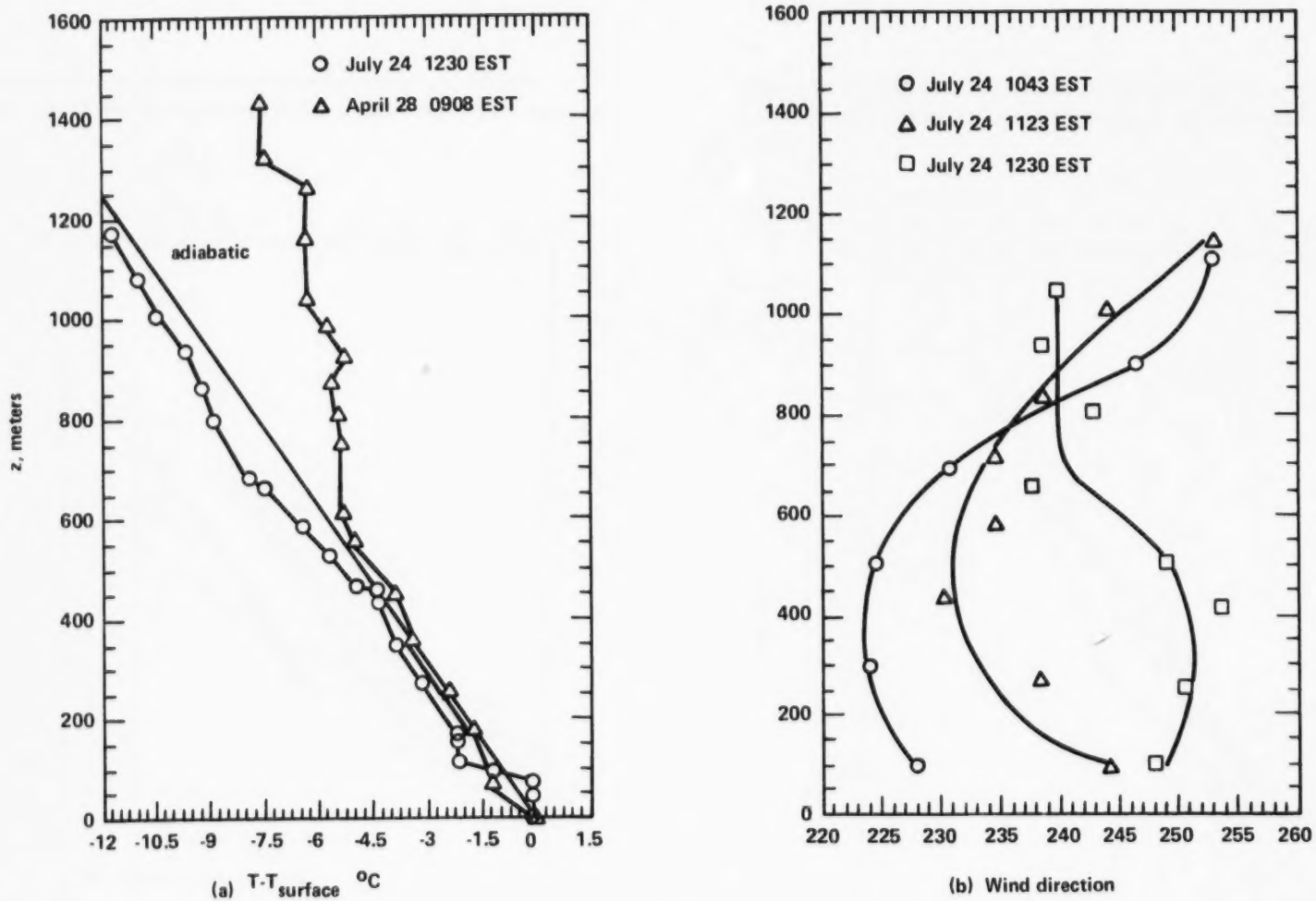

Figure 4. Temperature (a) and wind direction (b) from field pibal releases.

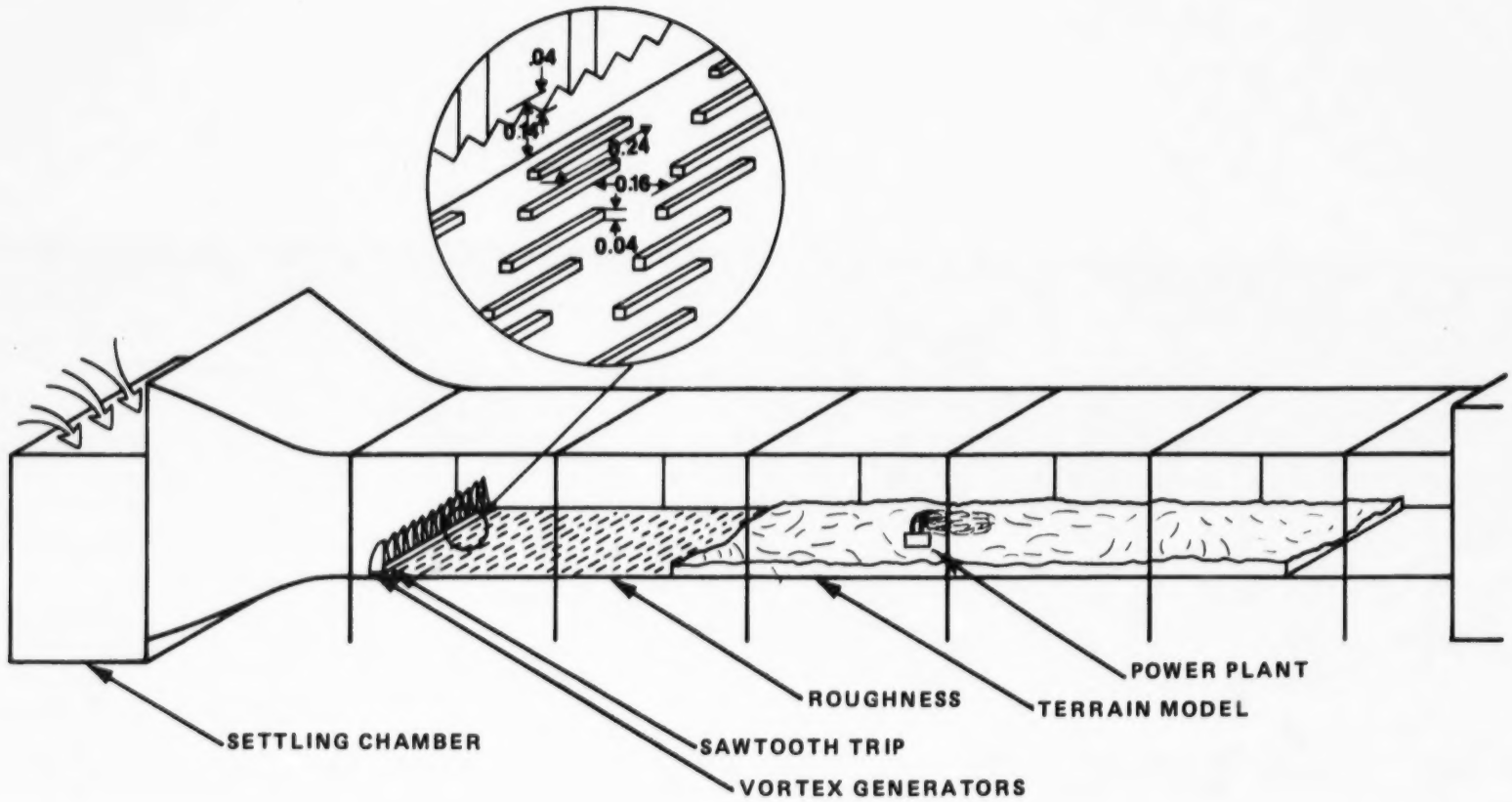

Figure 5. Schematic of the model in the wind-tunnel test section showing the vortex generators, trip and roughness for boundary-layer generation, and settling chamber.

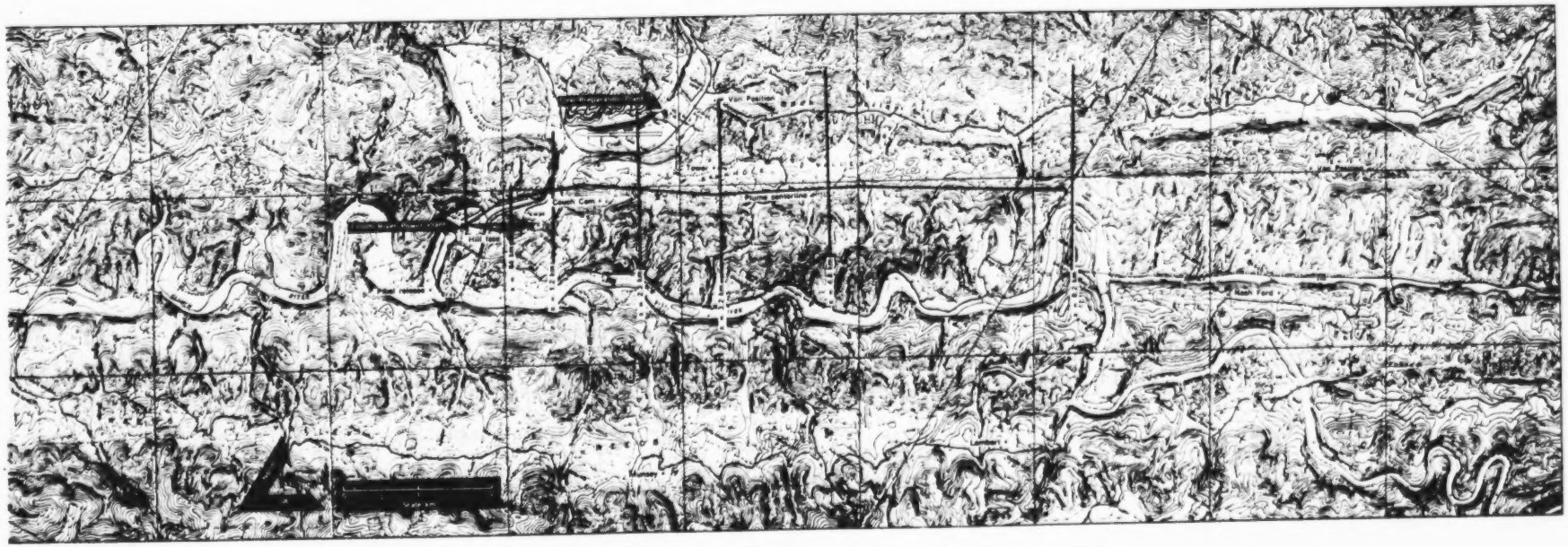

Figure 6. Topographical map of the area modeled. Locations of field sites and wind-tunnel sampling positions are indicated.

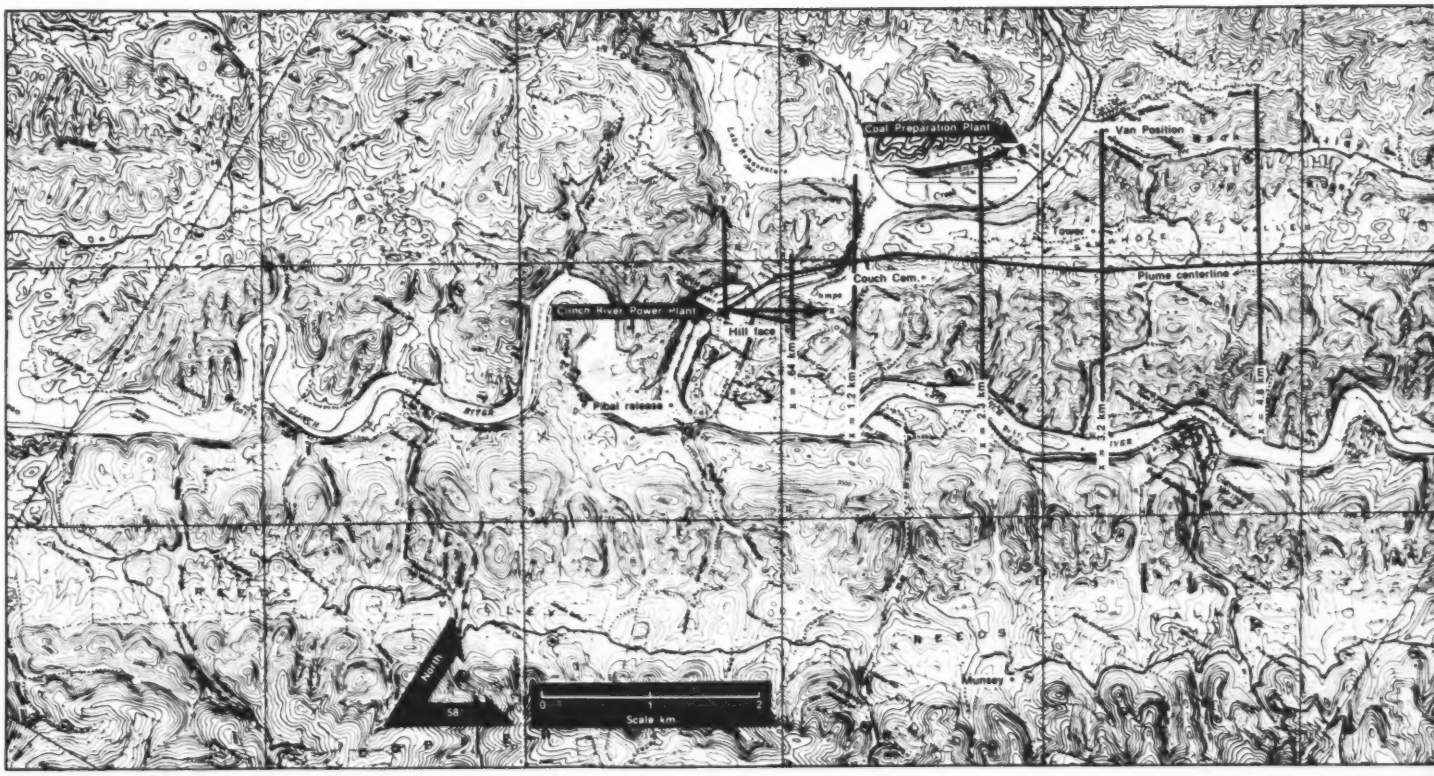

Figure 6. Topographical map of the area modeled. Locations of field sites and wind-tunnel samp

A

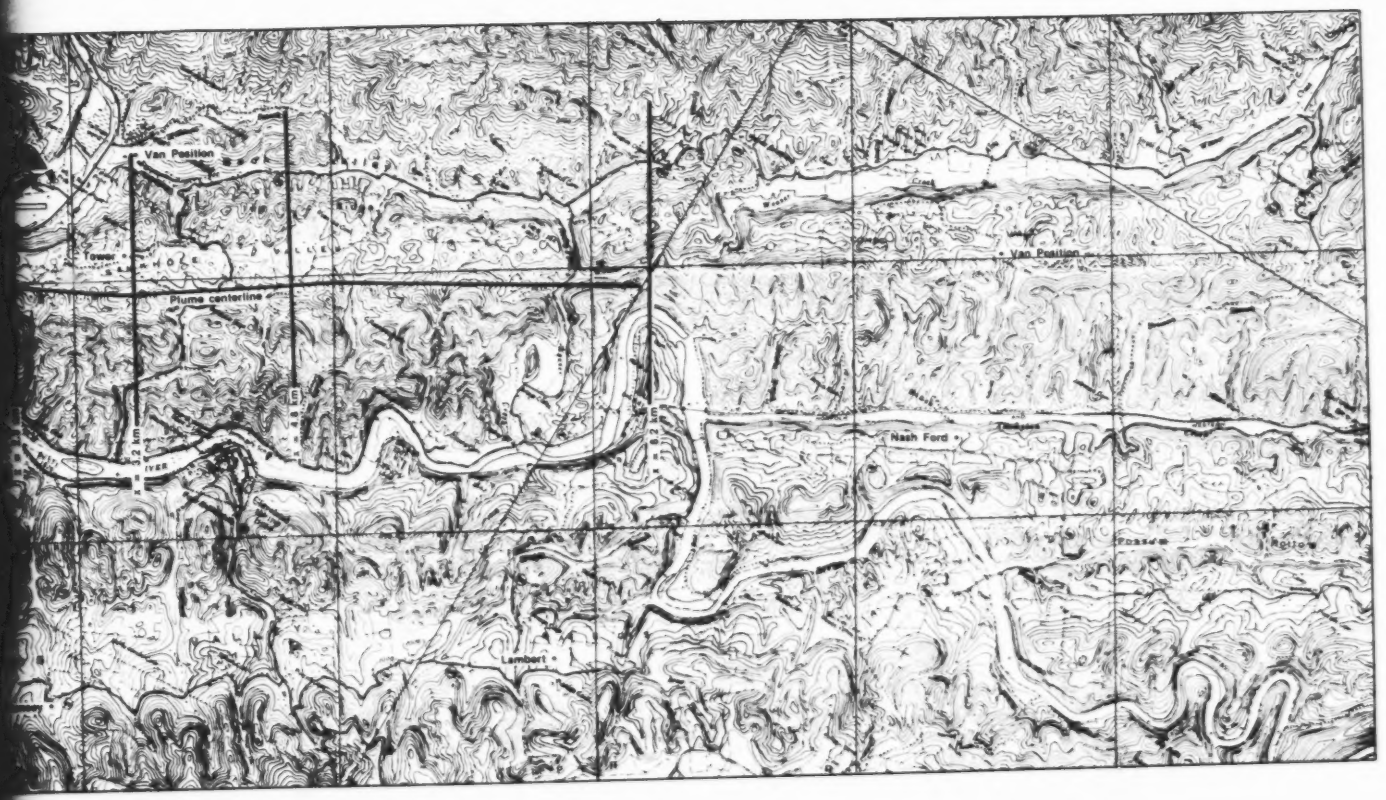

deled. Locations of field sites and wind-tunnel sampling positions are indicated.

B

Figure 7. The Clinch River terrain model in the wind tunnel. Vortex generators, sawtooth trip, and rows of roughness elements are upwind. Plant is in foreground.

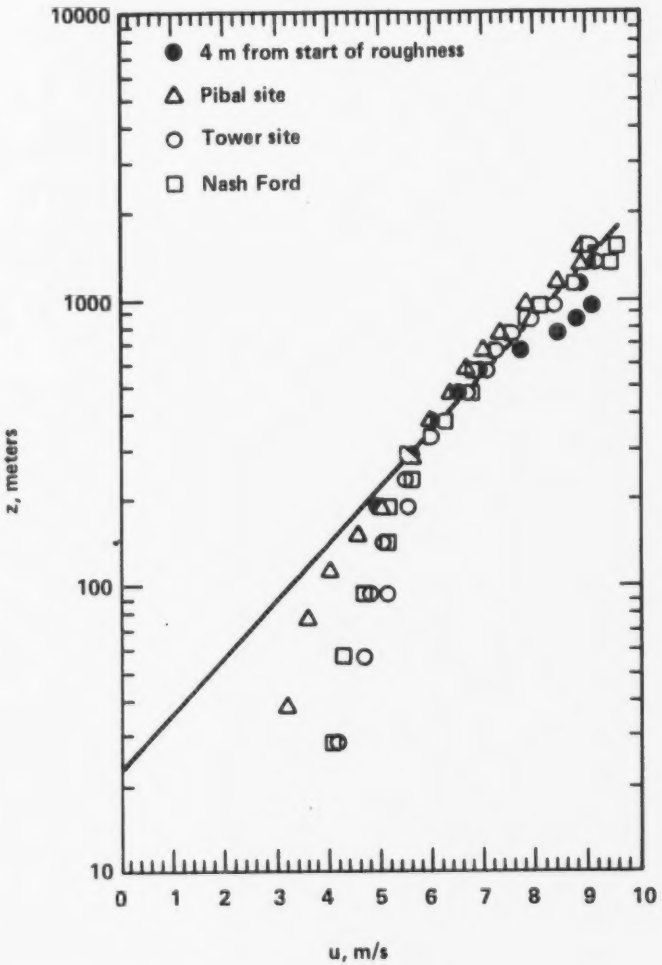

Figure 8. Mean velocity measurements at various longitudinal positions in the wind tunnel for July 24, 1000-1100 EST conditions.

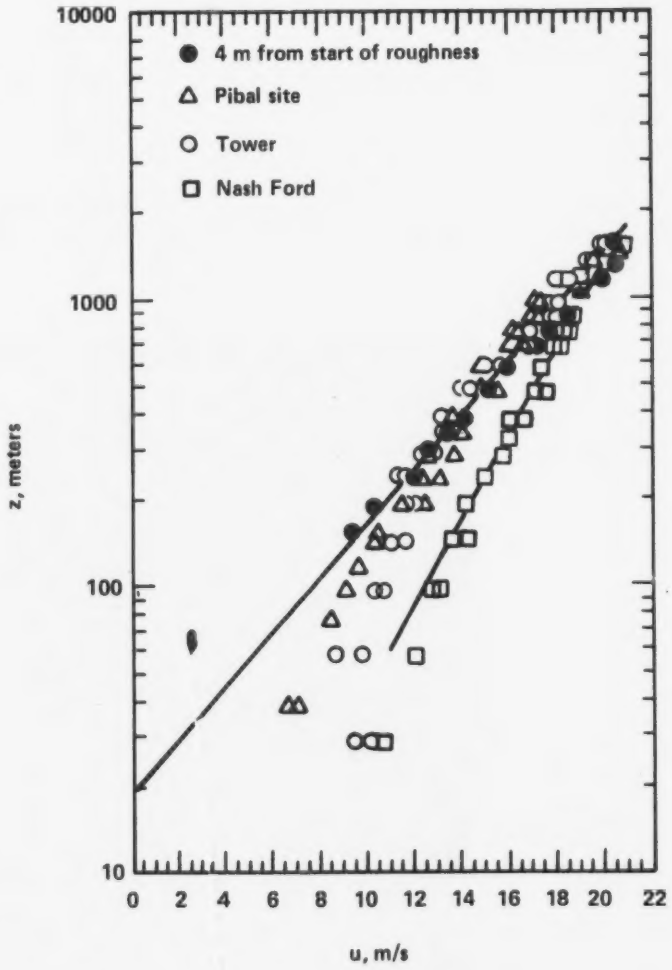

Figure 9. Mean velocity measurements at various longitudinal positions in the wind tunnel for April 28, 1800-1900 EST conditions.

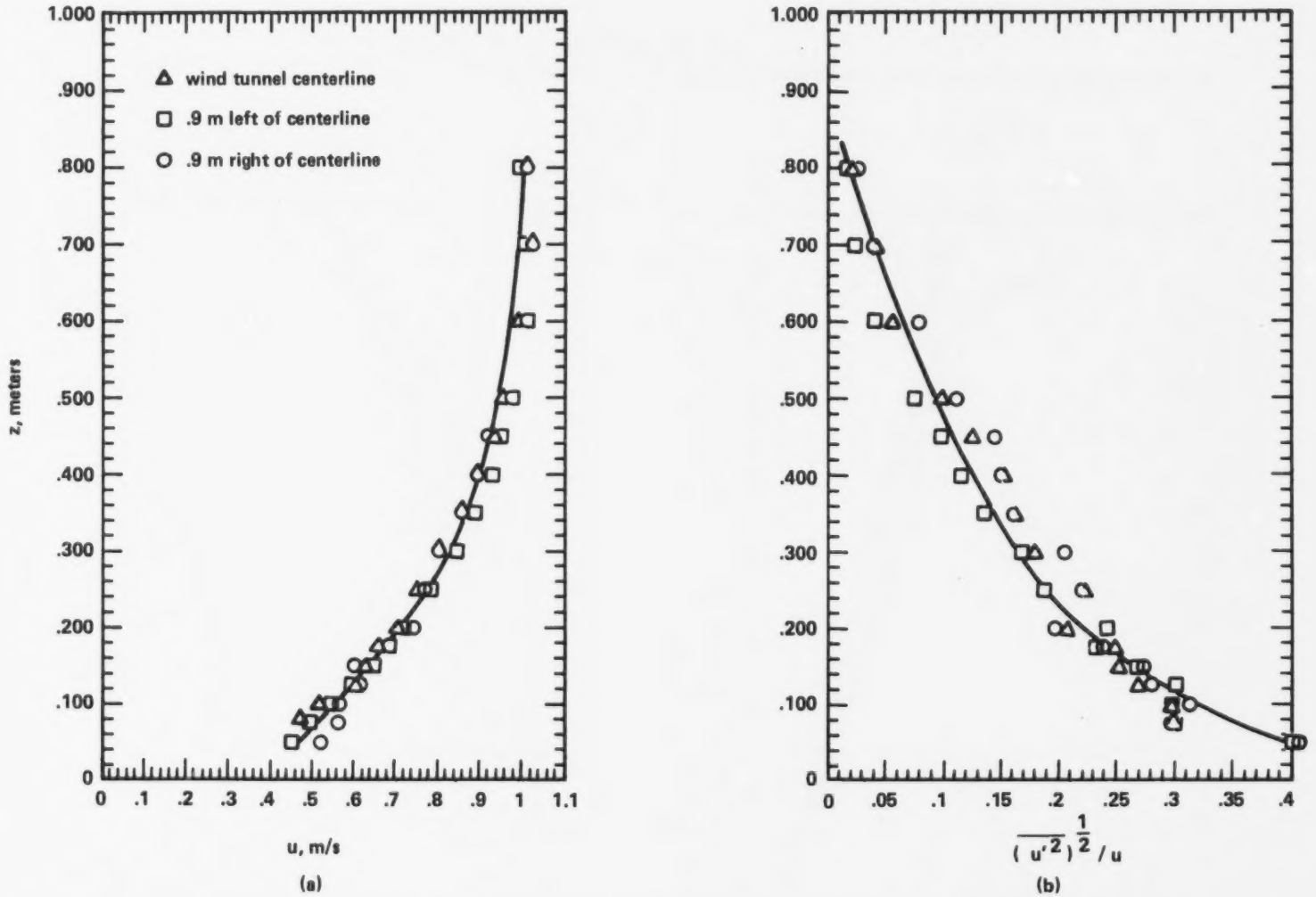

Figure 10. Lateral homogeneity of the approaching boundary-layer flow. Mean velocity (a) and turbulence intensity (b) at a distance of 4 meters from the upstream edge of the roughness. The velocity values are expressed in wind-tunnel units, $u_\infty = 1.0$ m/s.

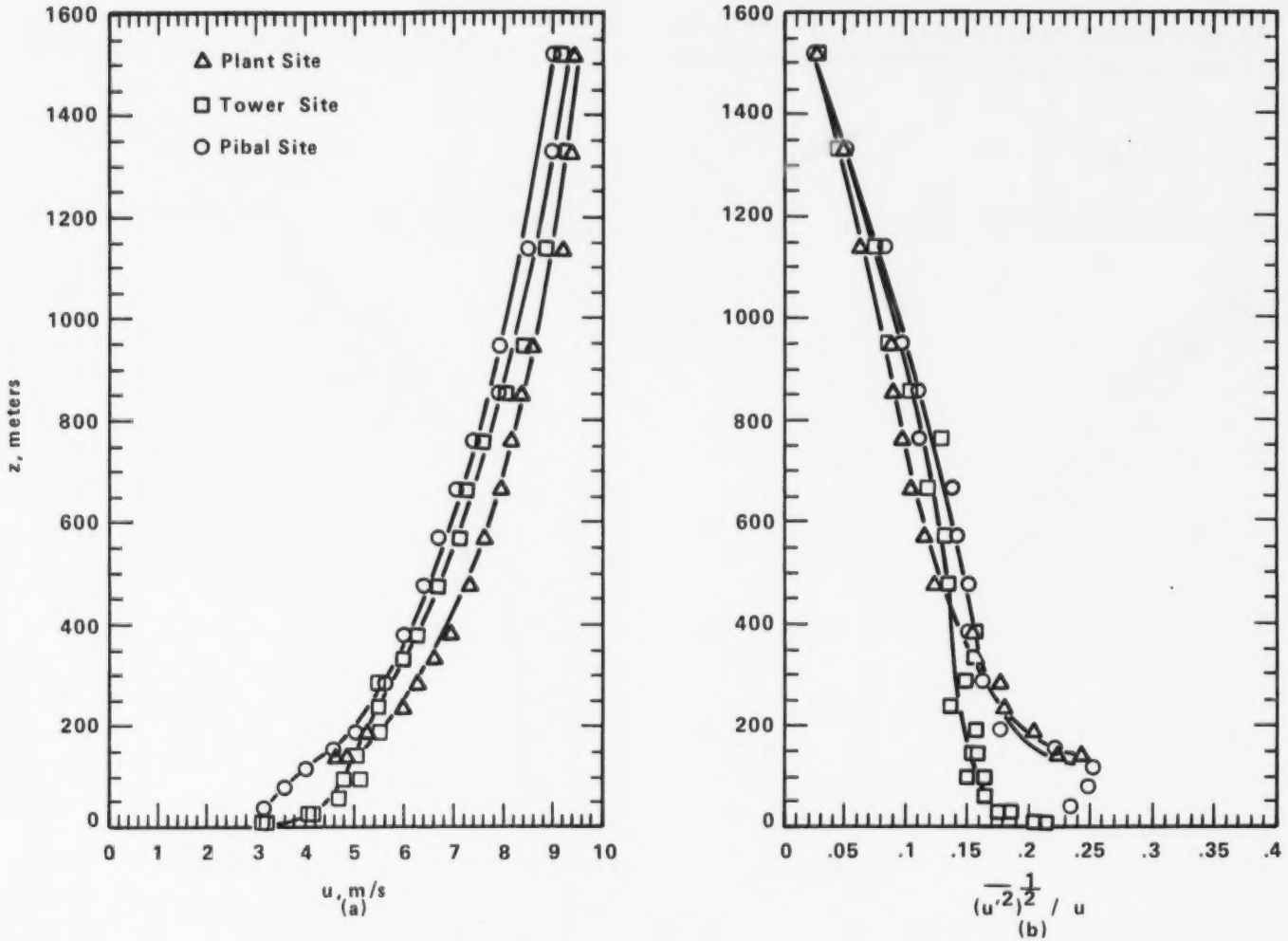

Figure 11. Mean velocity (a) and turbulence intensity (b) measured above Plant, Tower, and Pibal sites in the wind tunnel. Conditions modeled are July 24, 1000-1100 EST.

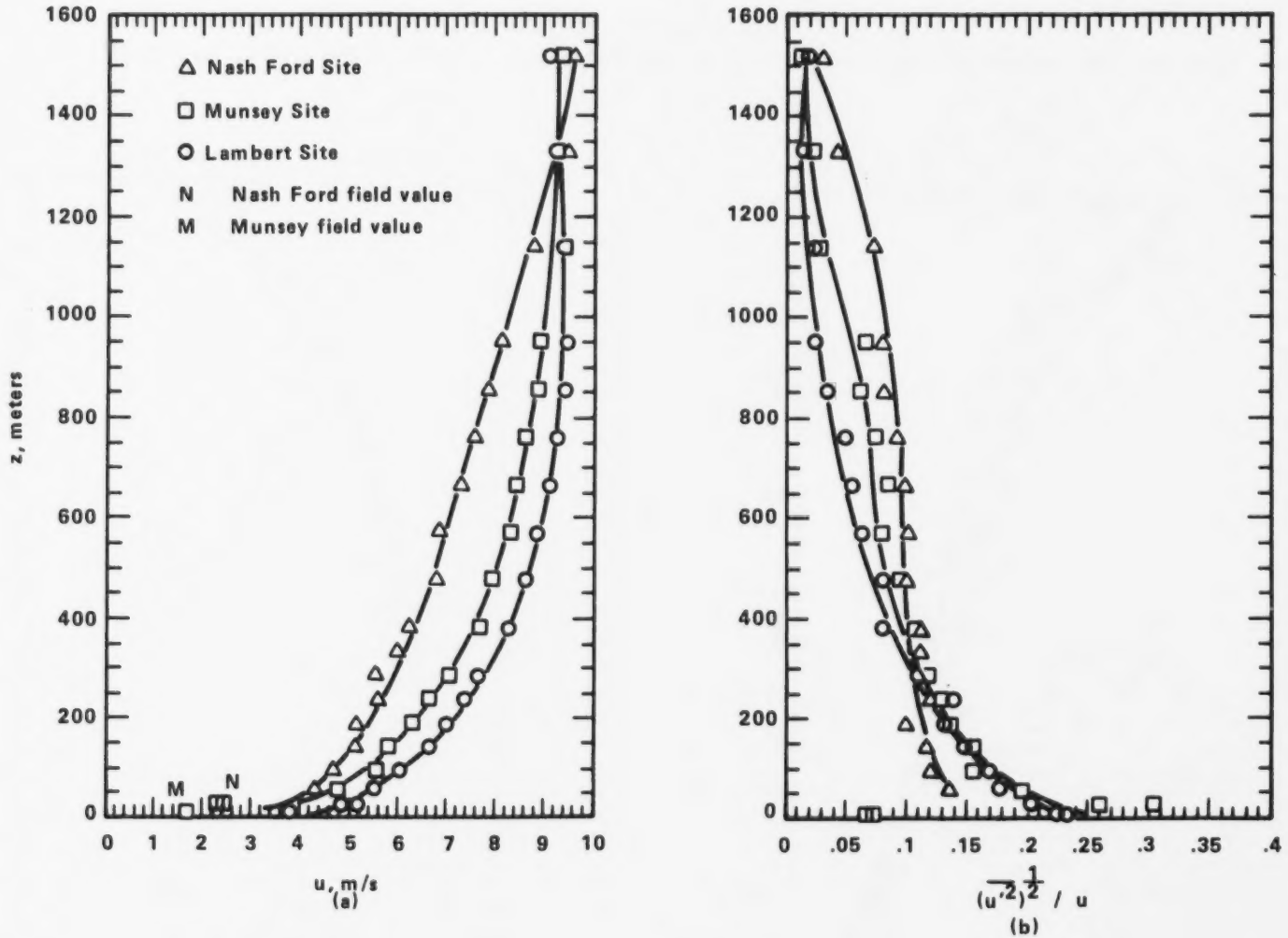

Figure 12. Mean velocity (a) and turbulence intensity (b) measured above Nash Ford, Munsey, and Lambert sites in the wind tunnel. Conditions modeled are July 24, 1000-1100 EST.

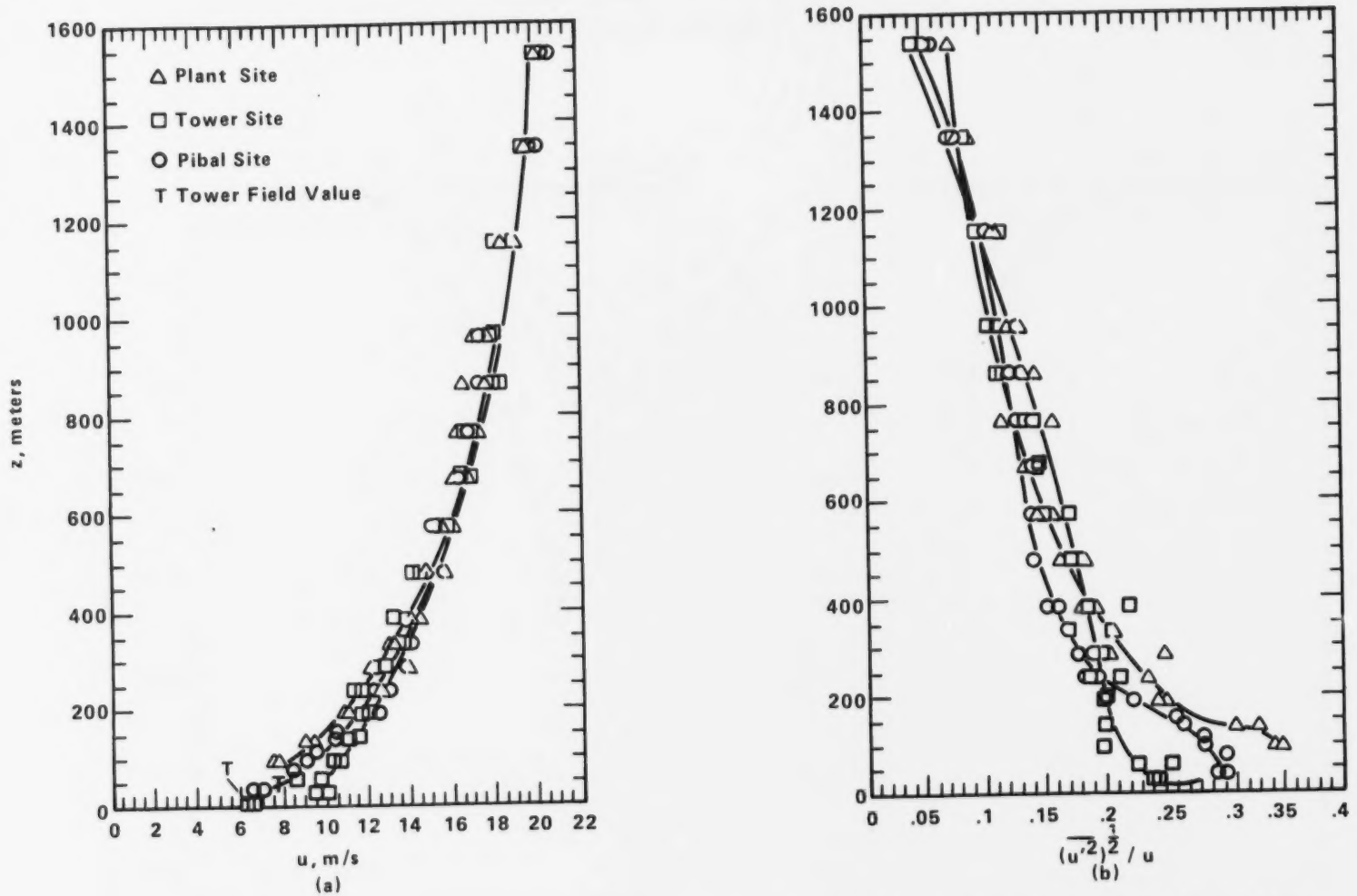

Figure 13. Mean velocity (a) and turbulence intensity (b) measured above Plant, Tower, and Pibal sites in the wind tunnel. Conditions modeled are April 28, 1800-1900 EST.

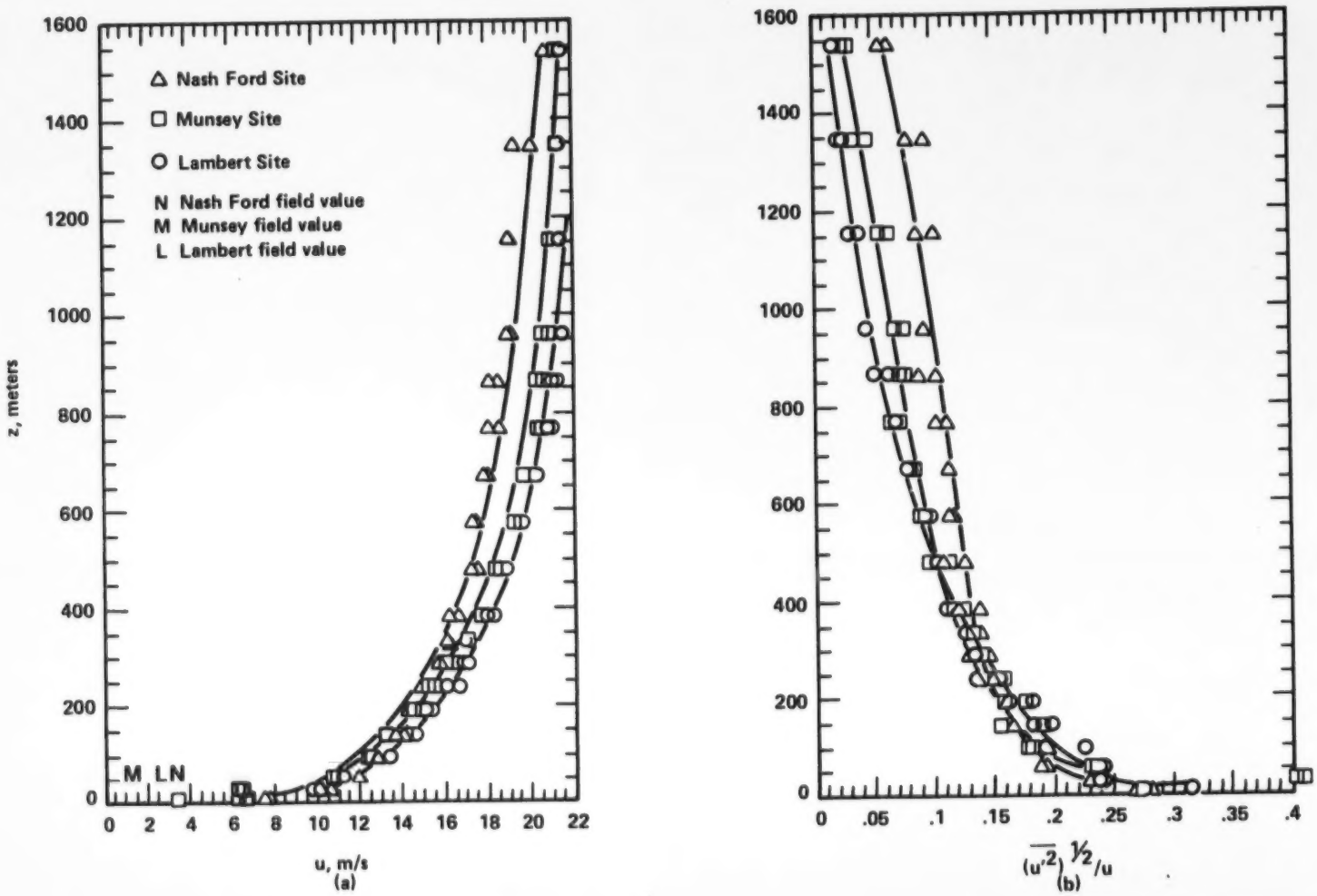

Figure 14. Mean velocity (a) and turbulence intensity (b) measured above Nash Ford, Munsey, and Lambert sites in the wind tunnel. Conditions modeled are April 28, 1800-1900 EST.

(a) 1023 EST

(b) 1025 EST

(c) 1027 EST

(d) 1029 EST

Figure 15. Photographs of the plume from one stack at the Clinch River Power Plant on July 24, 1977. (Courtesy of Geomet, Inc.)

(a) 1211 EST

(b) 1214 EST

(c) 1216 EST

(d) 1218 EST

Figure 16. Photographs of the plume from one stack at the Clinch River Power Plant on July 24, 1977. (Courtesy of Geomet, Inc.)

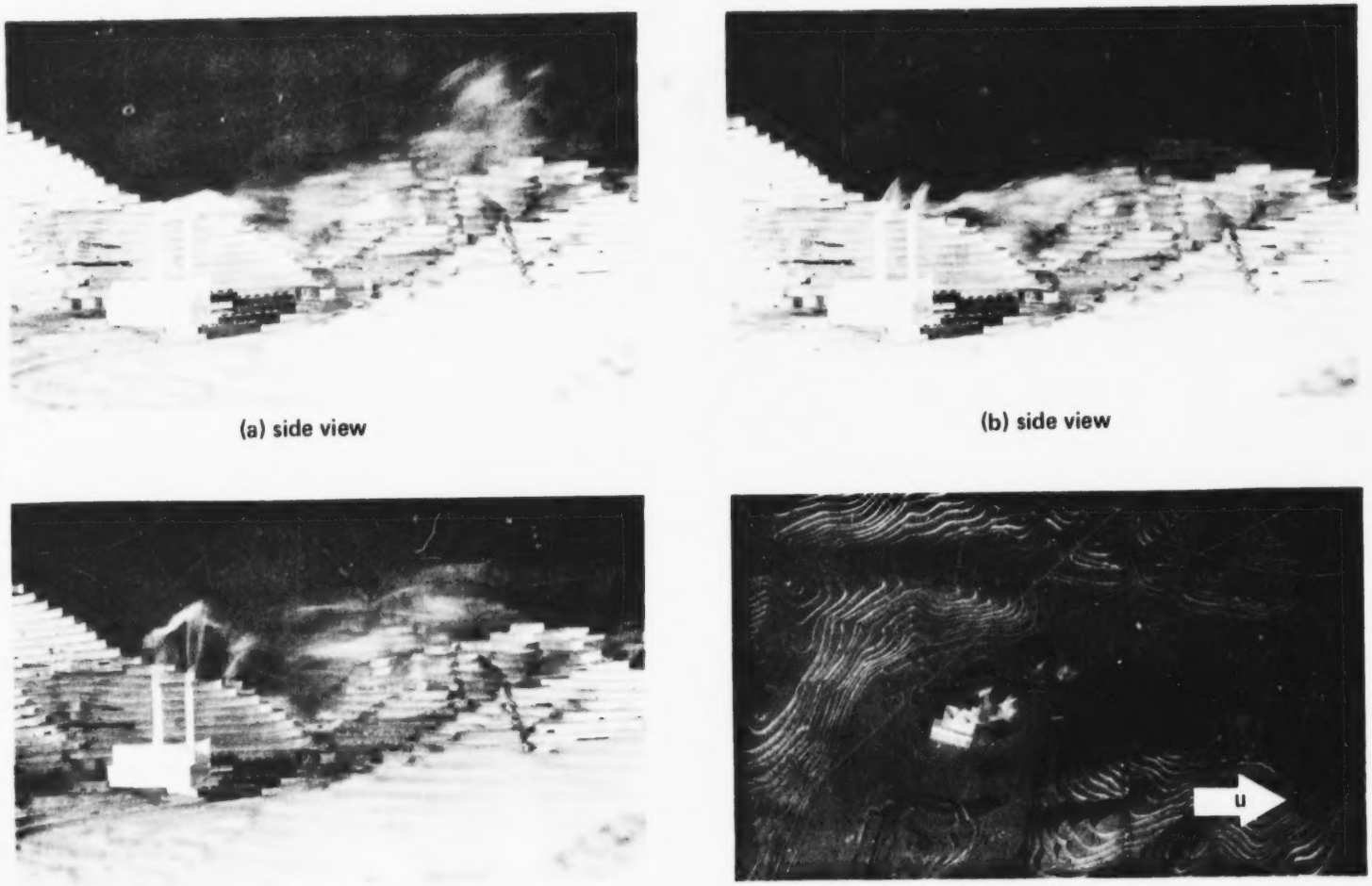

(a) side view

(b) side view

(c) side view

(d) top view

Figure 17. Flow visualization in the wind tunnel of July 24,1000-1100 EST conditions.

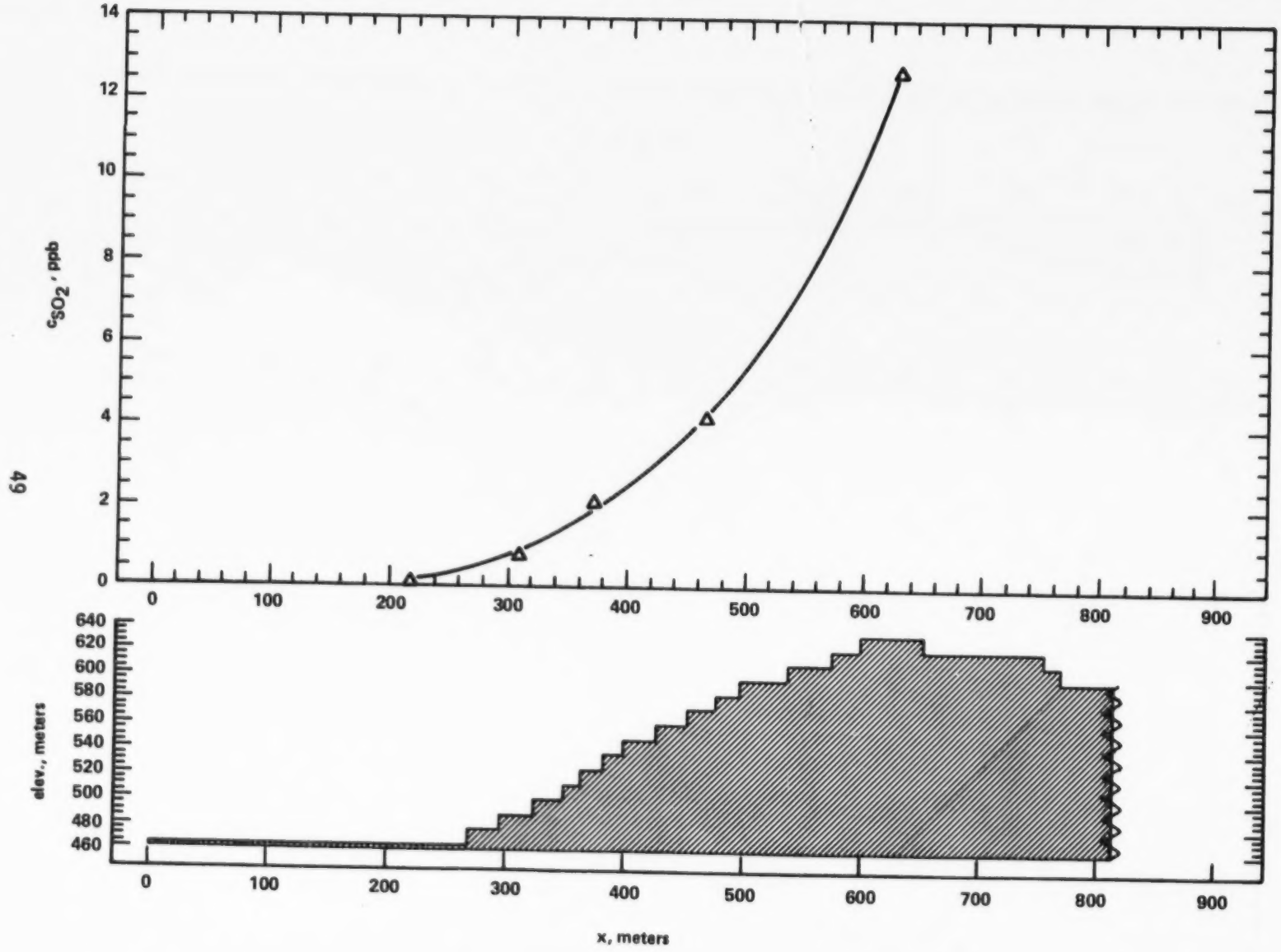

Figure 18. Ground-level concentrations on the face of the hill just downwind of the plant for July 24, 1000-1100 EST conditions.

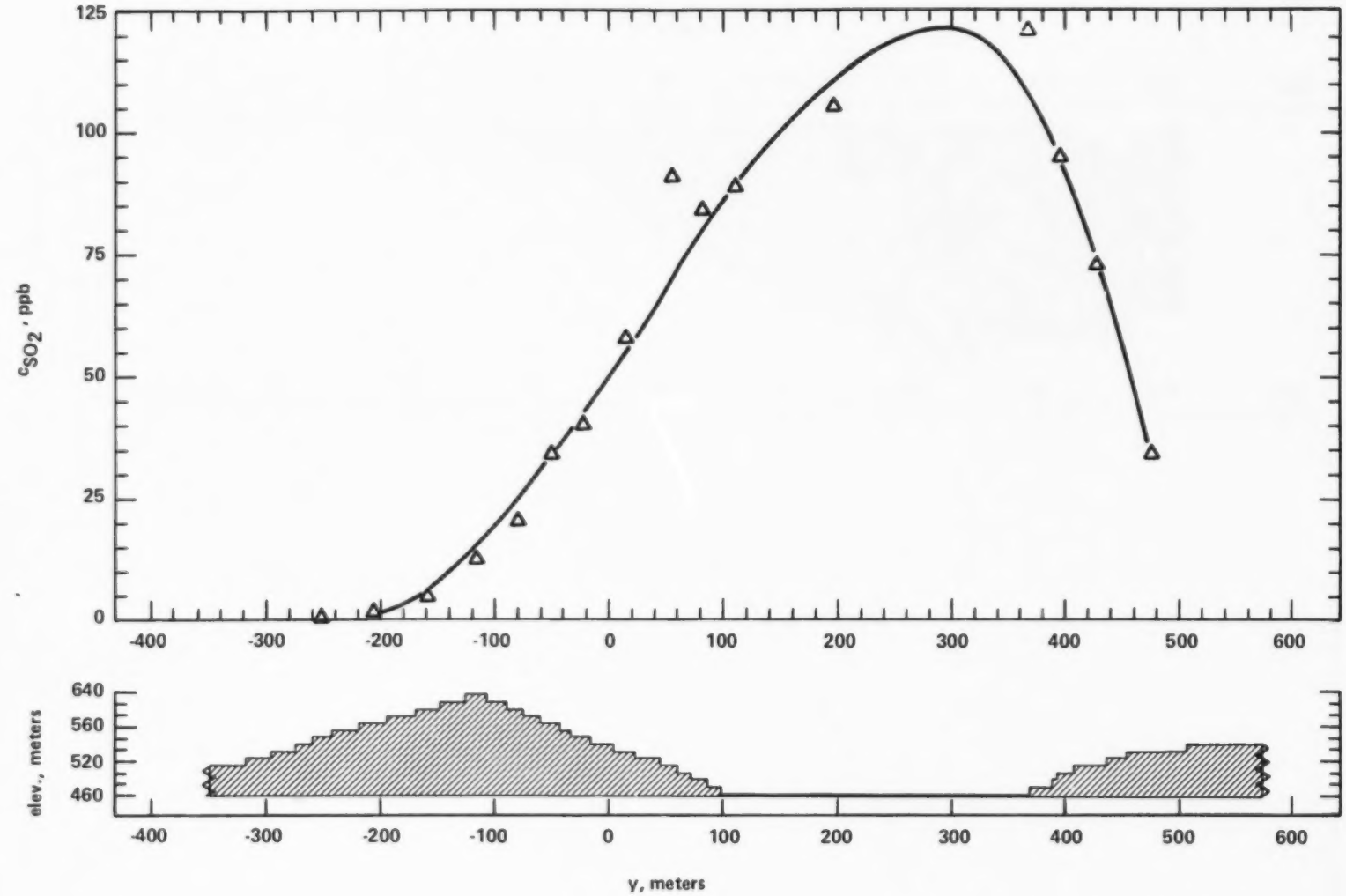

Figure 19. Ground-level concentrations at a distance of x = 0.64 km downwind of the stacks for July 24,1000-1100 EST conditions.

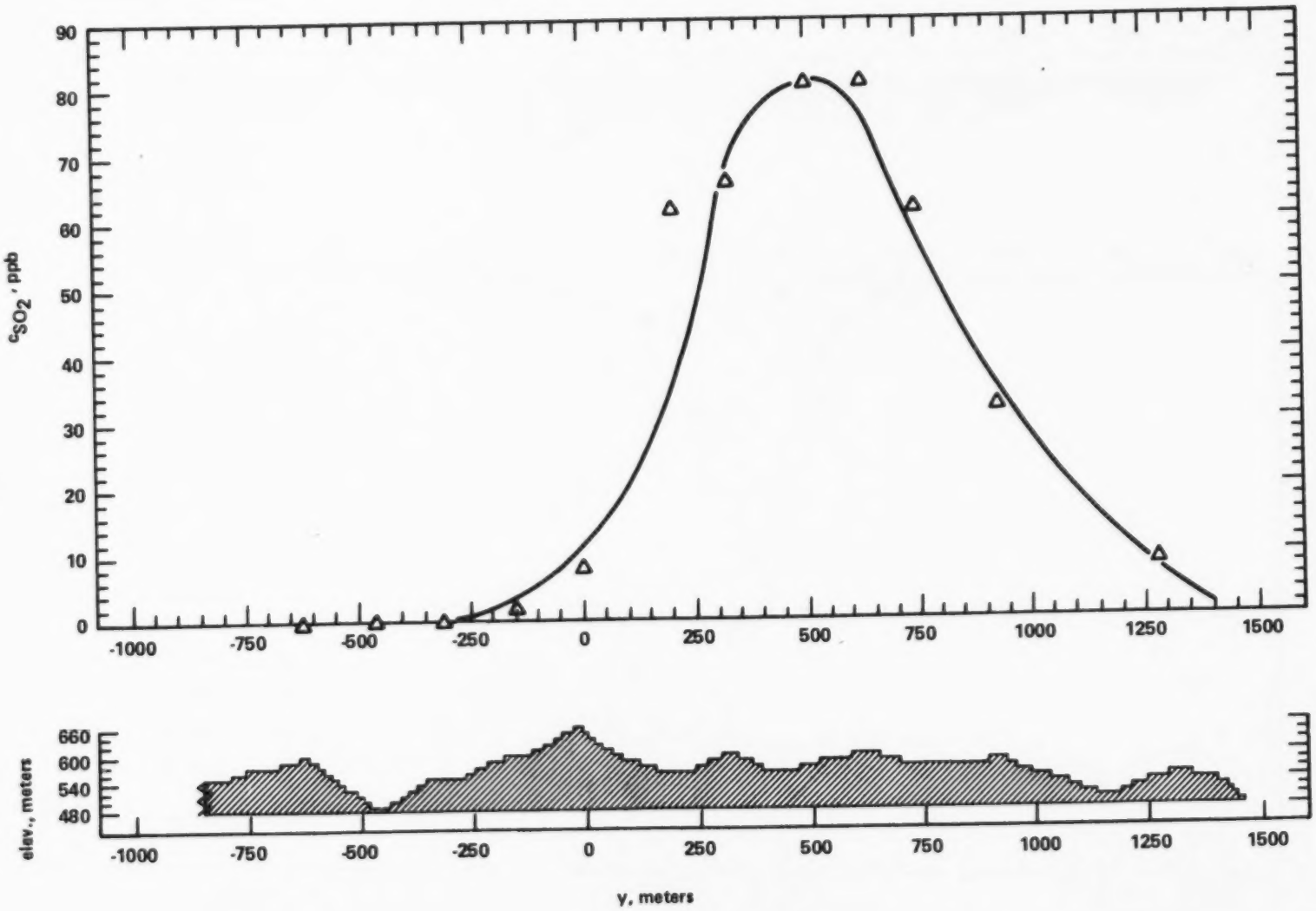

Figure 20. Lateral ground-level concentration profile at a distance of x = 3.2 km downwind of the stacks for July 24, 1000-1100 EST conditions.

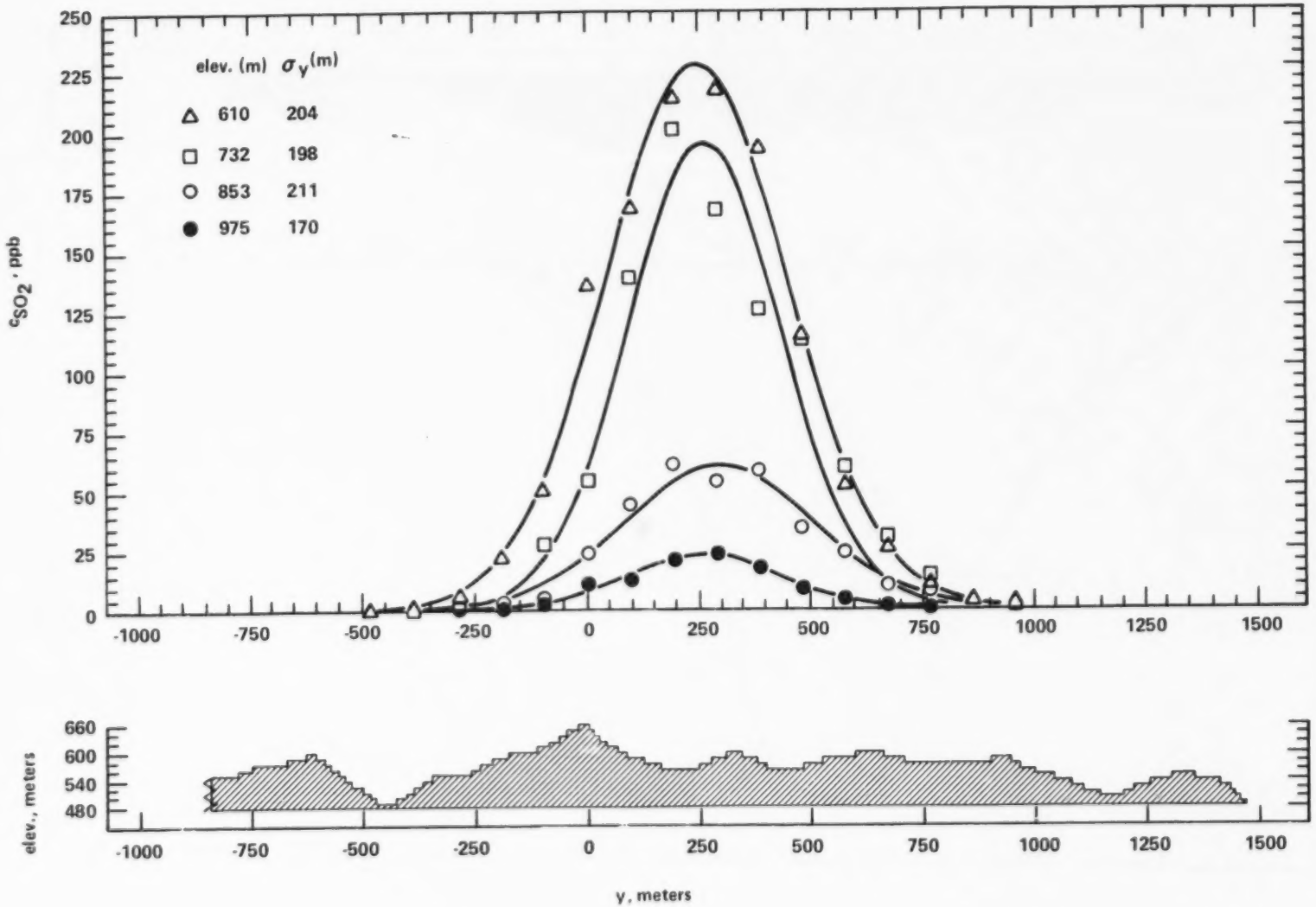

Figure 21. Lateral concentration profiles at a distance of x = 1.2 km downwind of the stacks for July 24, 1000-1100 EST conditions. Gaussian curve fits are drawn with the σ_y's specified.

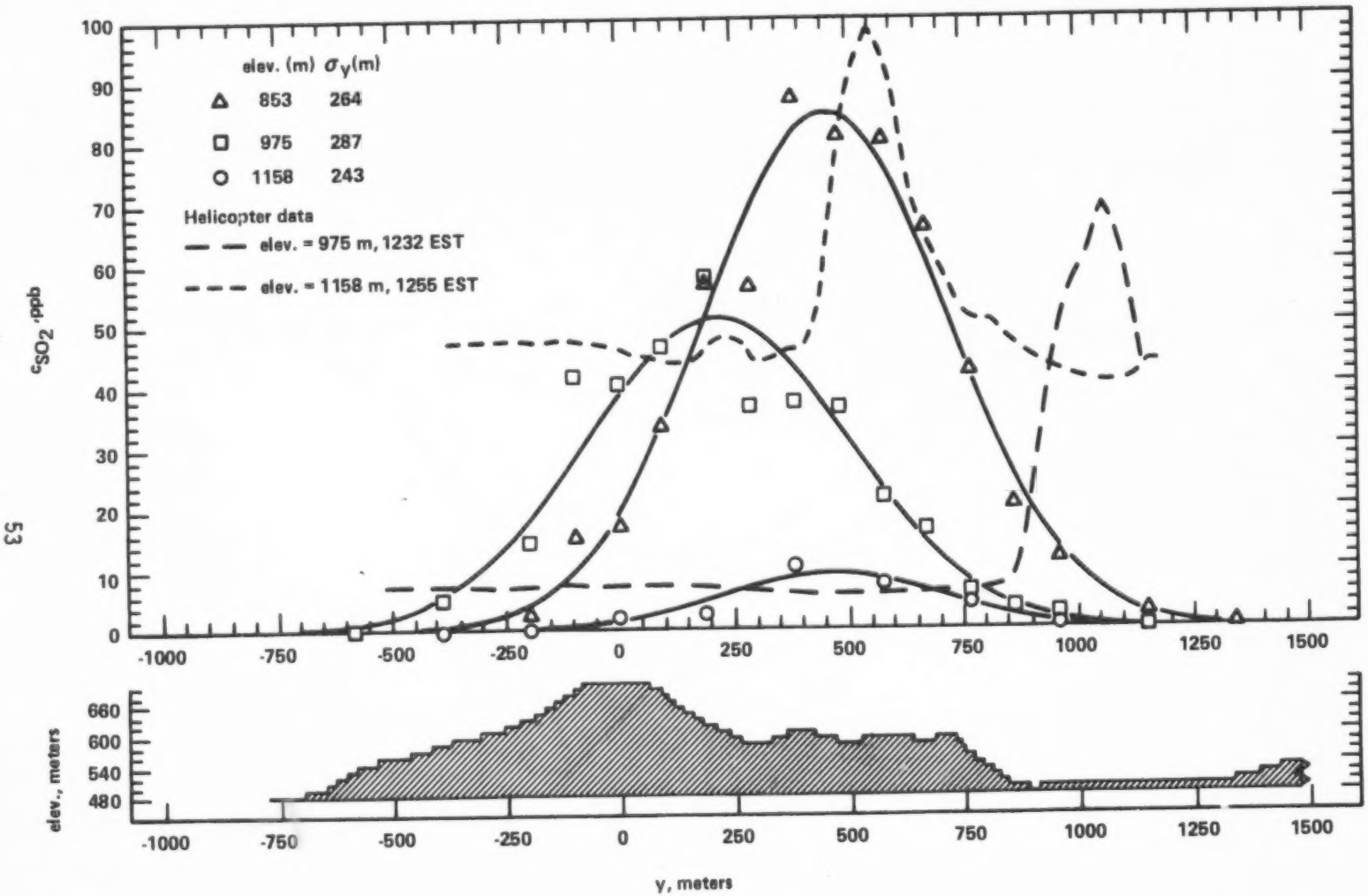

Figure 22. Lateral concentration profiles at a distance of x = 2.3 km downwind of the stacks for July 24, 1000-1100 EST conditions. Gaussian curve fits are drawn with the σ_y's specified. Field helicopter data are also shown for slightly later sampling period.

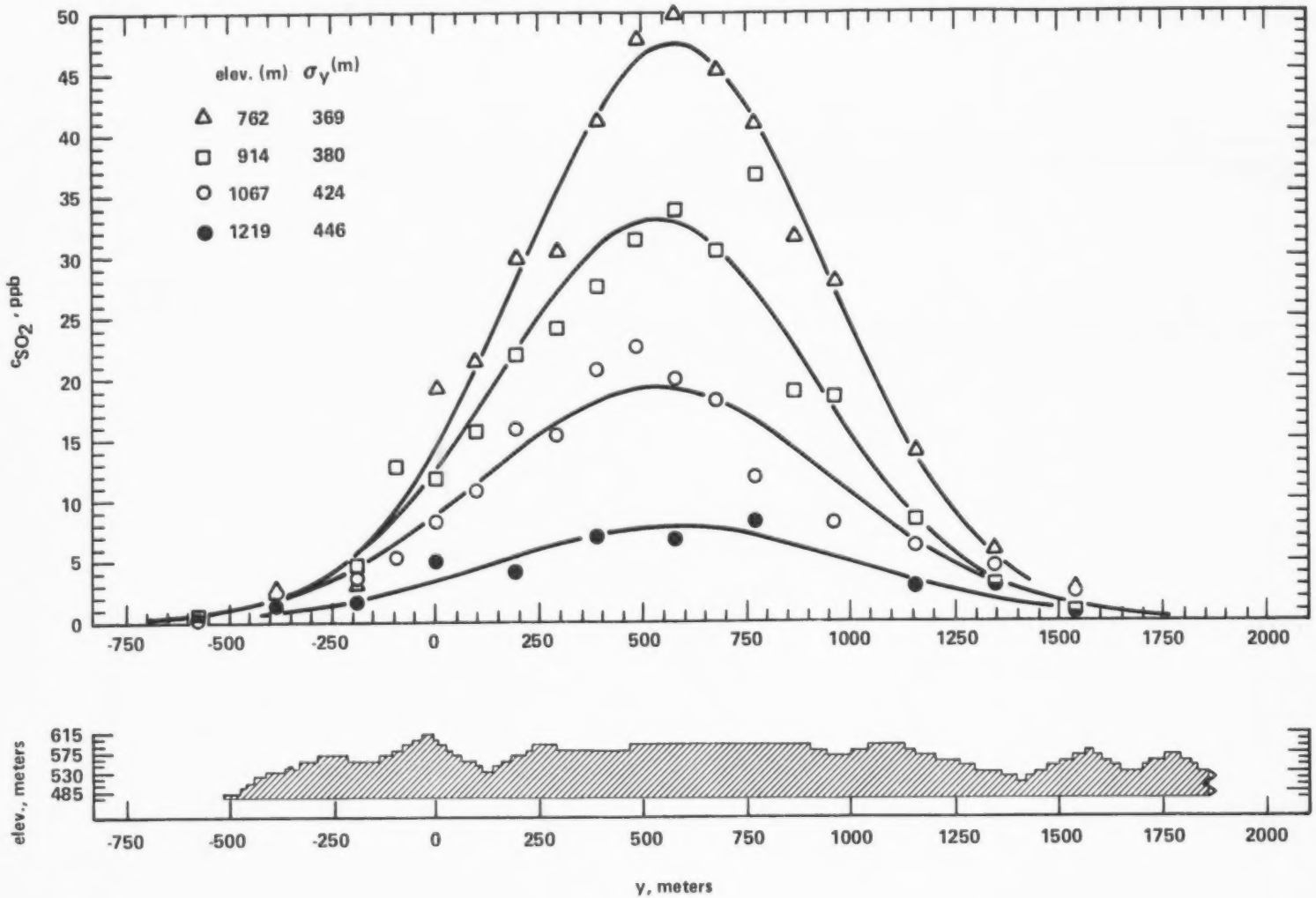

Figure 23. Lateral concentration profiles at a distance of x = 4.8 km downwind of the stacks for July 24, 1000-1100 EST conditions. Gaussian curve fits are drawn with the σ_y's specified.

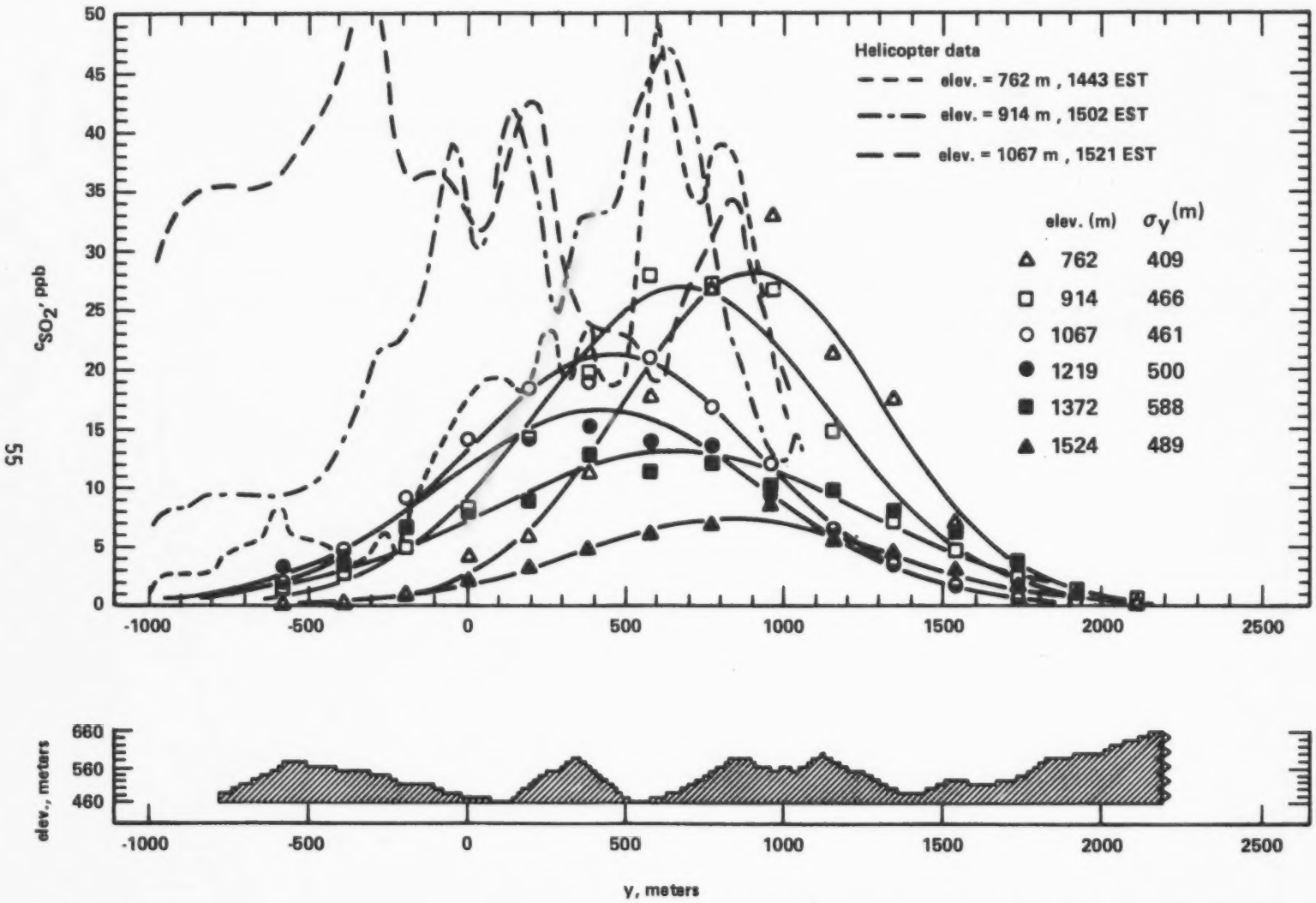

Figure 24. Lateral concentration profiles at a distance of x = 8.2 km downwind of the stacks for July 24, 1000-1100 EST conditions. Gaussian curve fits are drawn with the σ_y's specified. Field helicopter data are also shown for slightly later sampling period.

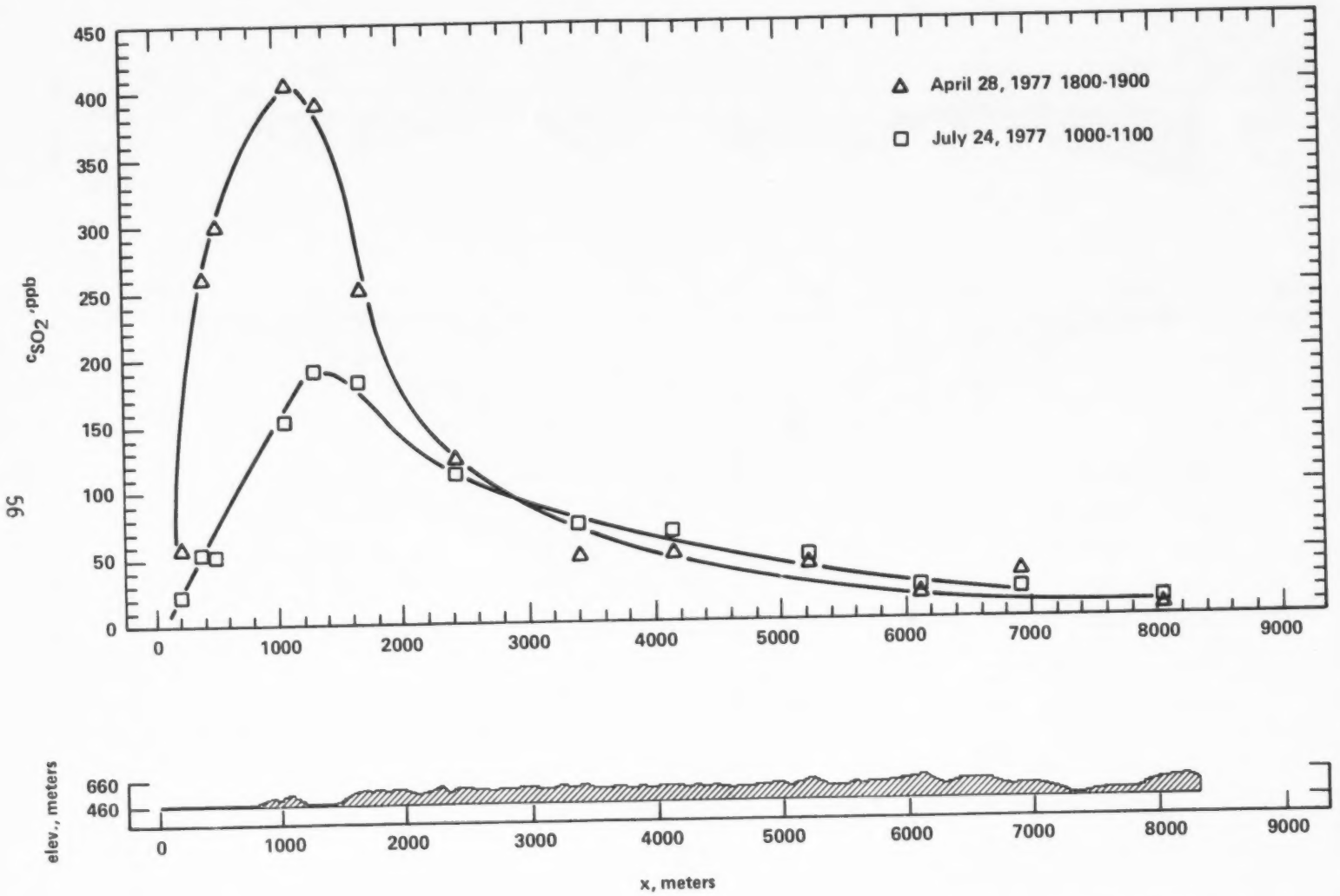

Figure 25. Ground-level concentrations under the plume centerline (Figure 6) for July 24, 1000-1100 EST conditions and April 28, 1800-1900 conditions.

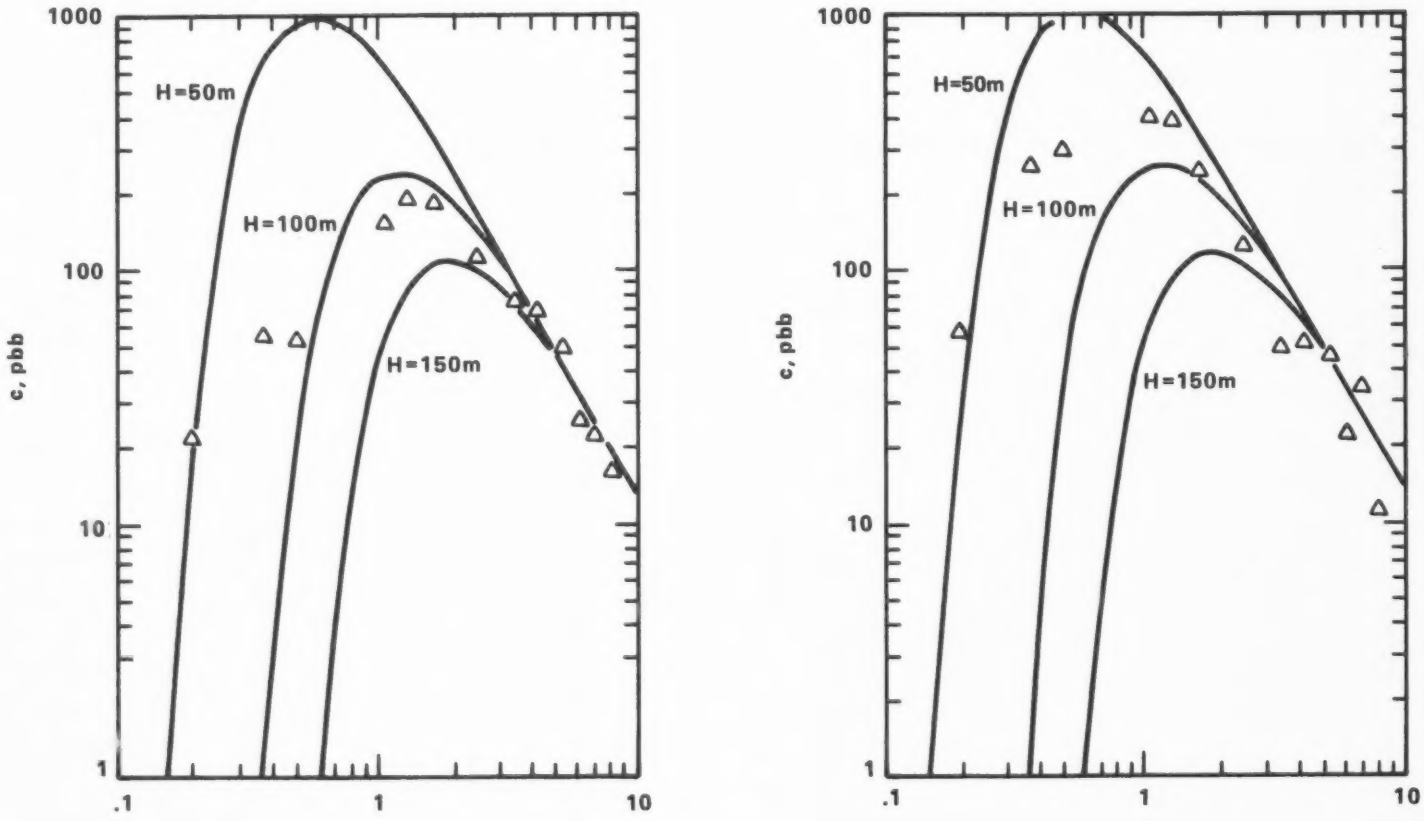

Figure 26. Ground-level concentrations measured under plume centerline in wind tunnel compared with flat-terrain Gaussian model: $c=(Q/\pi\sigma_y\sigma_z u)\exp(-\frac{1}{2}(H/\sigma_z)^2)$, with σ_y and σ_z calculated for C stability.

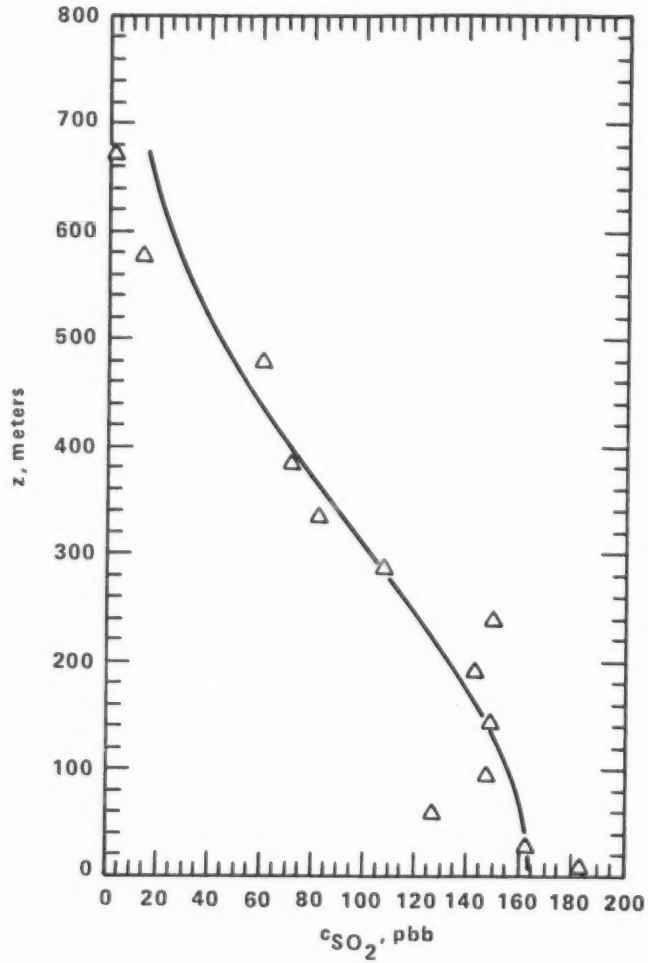

Figure 27. Vertical concentration profile above Couch Cemetery for July 24 conditions, x = 1.65 km. Gaussian σ_z = 290 m.

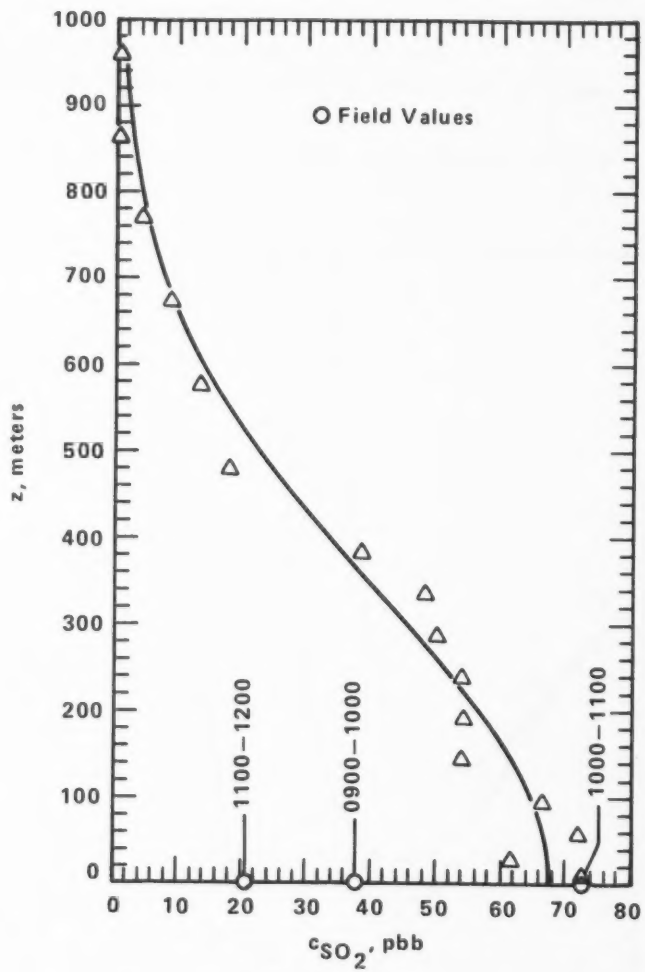

Figure 28. Vertical concentration profile above Tower site for July 24 conditions, x = 3.2 km. Gaussian σ_z = 318 m.

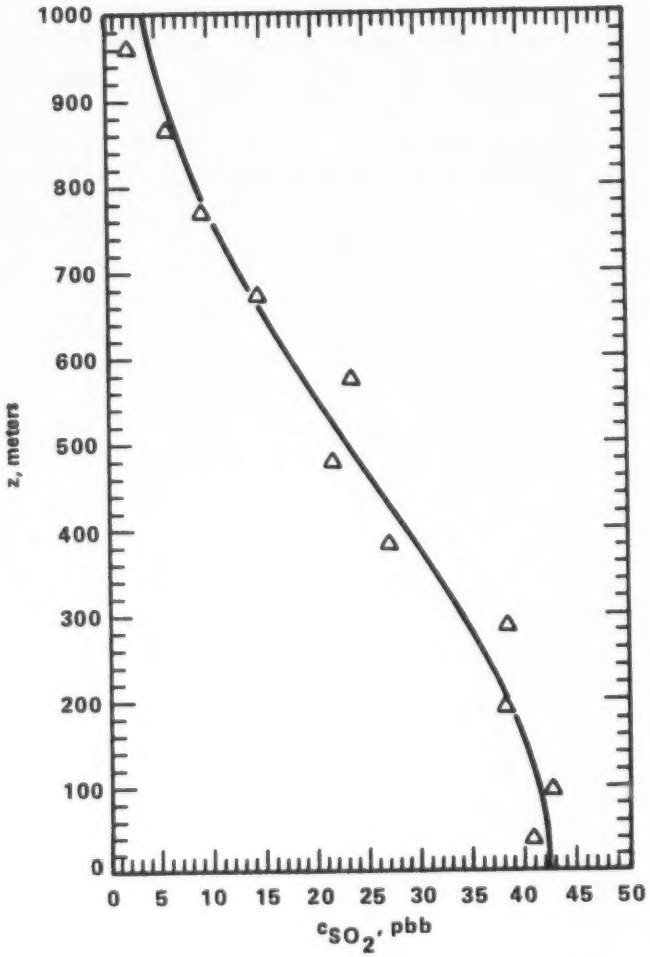

Figure 29. Vertical concentration profile for July 24 conditions, x = 4.8 km, y = 0.4 km. Gaussian σ_z = 439 m.

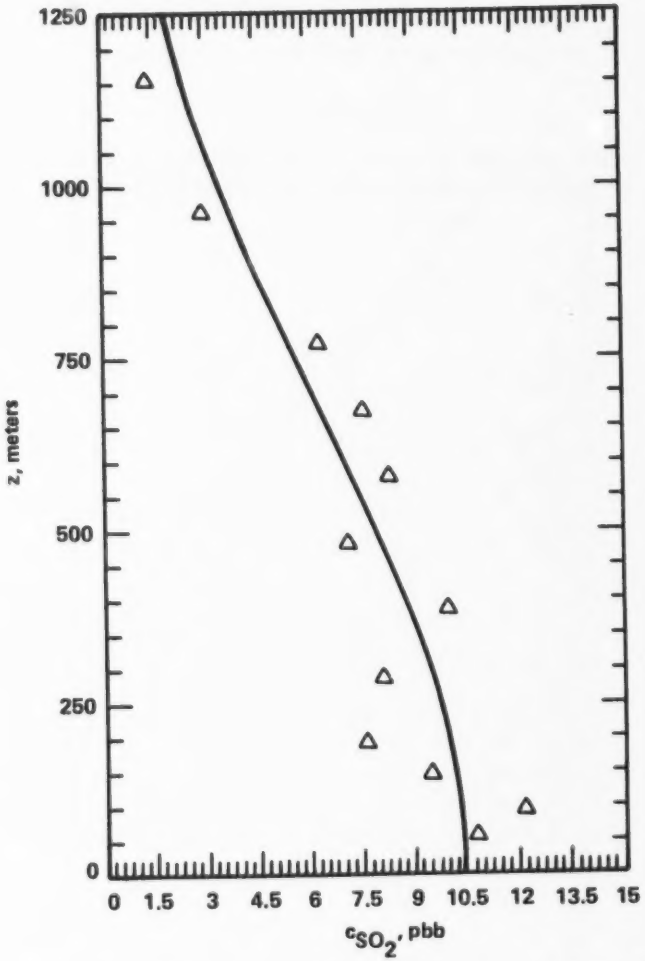

Figure 30. Vertical concentration profile for July 24 conditions, x = 8.2 km, y = 0.4 km. Gaussian σ_z = 659 m.

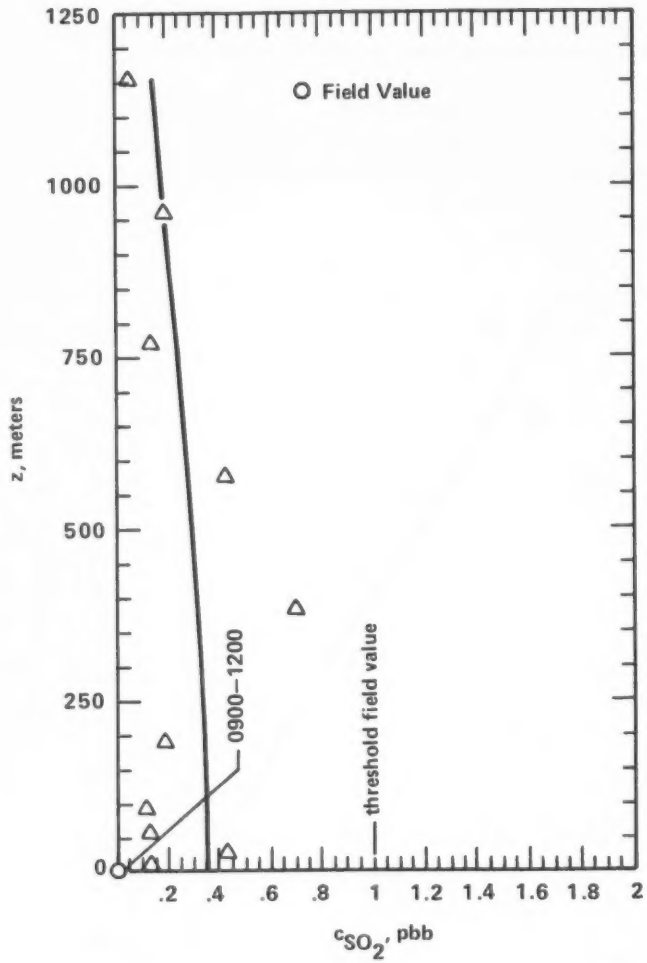

Figure 31. Vertical concentration profile above Nash Ford site for July 24 conditions, x = 10.2 km. Gaussian σ_z = 857 m.

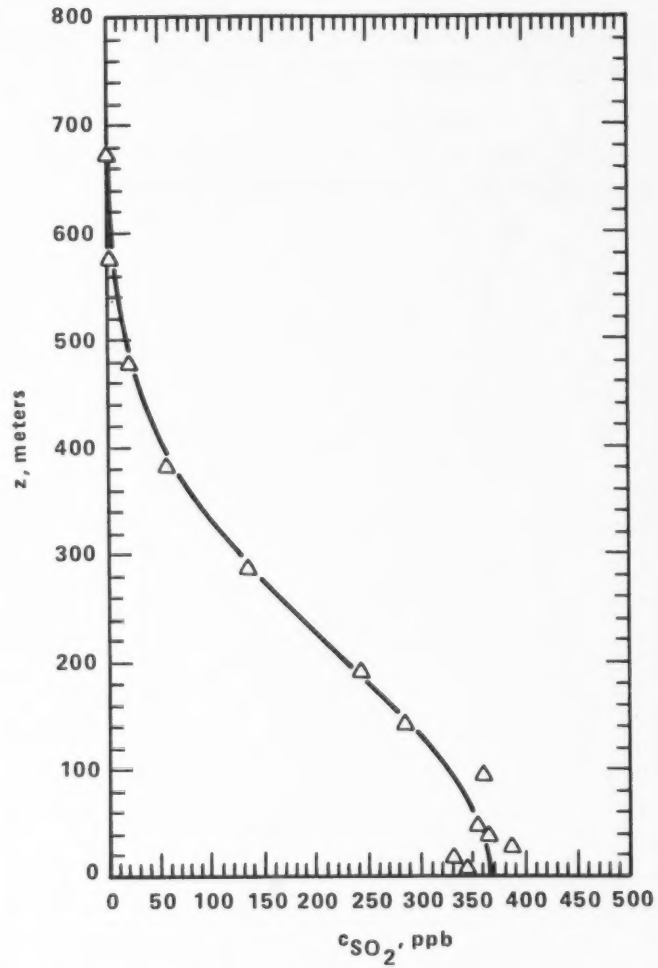

Figure 32. Vertical concentration profile for April 28 conditions, x = 1.2 km, y = 0.4 km. Gaussian σ_z = 192 m.

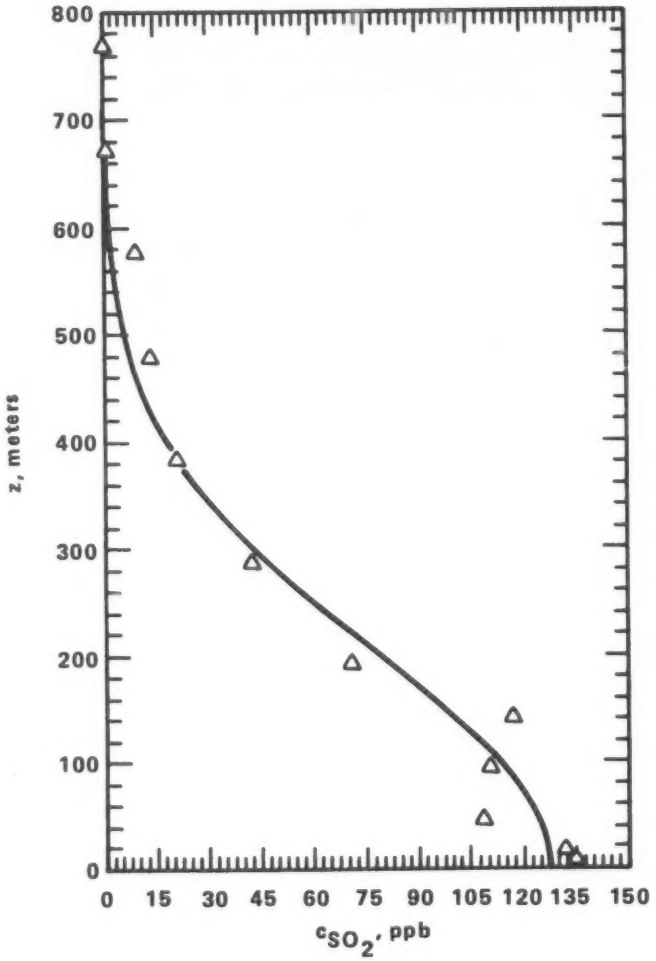

Figure 33. Vertical concentration profile for April 28 conditions, x = 2.3 km, y = 0.4 km. Gaussian σ_z = 187 m.

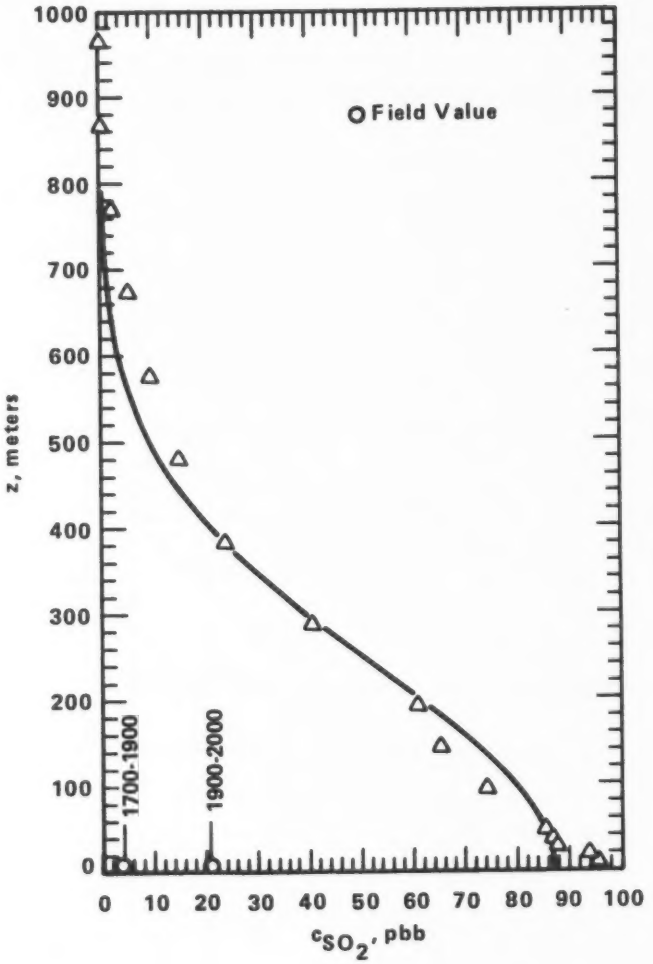

Figure 34. Vertical concentration profile above Tower site for April 28 conditions, x = 3.2 km. Gaussian σ_z = 225 m.

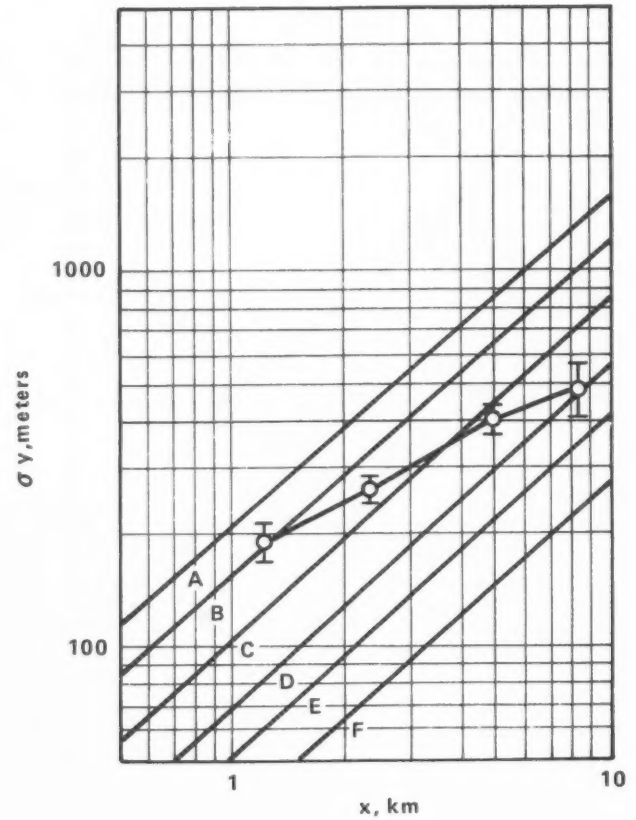

Figure 35. Wind-tunnel σ_y values for July 24 test conditions as compared with Pasquill-Gifford values.

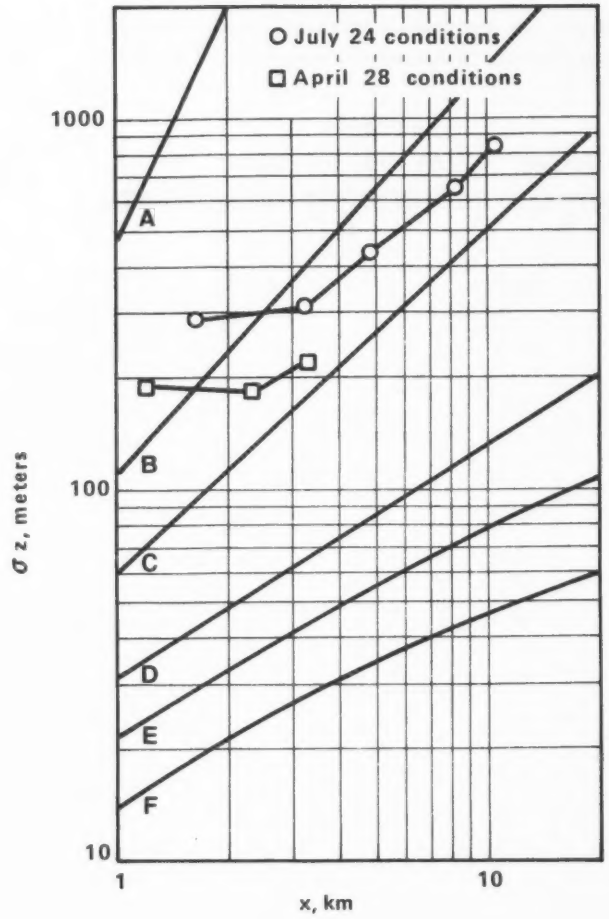

Figure 36. Wind-tunnel σ_z values as compared with Pasquill-Gifford values.